

Edith Cowan University
Research Online

ECU Publications Pre. 2011

2006


The Hillarys Transect (1): Seasonal and cross-shelf variability of physical and chemical water properties off Perth, Western Australia, 1996-98

Alan Pearce

Mervyn Lynch

Christine Hanson
Edith Cowan University

Follow this and additional works at: <https://ro.ecu.edu.au/ecuworks>

 Part of the [Oceanography Commons](#), and the [Terrestrial and Aquatic Ecology Commons](#)

10.1016/j.csr.2006.05.008

Revised manuscript for Continental Shelf Research (ISSN: 0278-4343) click [here](#) for publication home page and article index

This Journal Article is posted at Research Online.
<https://ro.ecu.edu.au/ecuworks/2200>

The Hillarys Transect (1): Seasonal and cross-shelf variability of physical and
chemical water properties off Perth, Western Australia, 1996-98

A.F. Pearce^{*,1}, M.J. Lynch² and C.E. Hanson^{1,3}

¹CSIRO Marine Research, Private Bag 5, Wembley, Western Australia 6913, Australia.

E-mail: alan.pearce@csiro.au

*Corresponding author; Ph +618 9333 6510, Fax +618 9333 6555

²Curtin University of Technology, Bentley, Western Australia 6845, Australia.

E-mail: m.lynch@curtin.edu.au

³Centre for Ecosystem Management, Edith Cowan University, 100 Joondalup Drive, Joondalup,
Western Australia 6027, Australia. E-mail: c.hanson@ecu.edu.au

Revised manuscript for *Continental Shelf Research*

April 2006

Abstract

2 A 27-month study of the water properties across the continental shelf off Perth, Western
Australia (the "Hillarys Transect") has provided the first systematic inter-disciplinary
4 climatology of the physical, chemical, optical and biological cycles across the shelf. This paper
describes the main features of the seasonal and cross-shelf variability of the physical
6 oceanography and chemistry, while companion papers discuss some of the links between the
biology and physics of the region.

8 The oceanography is dominated by the seasonally-varying Leeuwin Current flowing
southwards along the shelf break and outer shelf, and the northwards inshore Capes Current
10 which is driven by the net southerly wind stress between about October and March (the austral
summer). As a result of the poleward boundary current, there is no large-scale upwelling
12 comparable with the Humboldt and Benguela Current systems. Water temperature and salinity in
the shallow coastal waters are largely influenced by air-sea heat flux processes, while advection
14 plays a more important role along the outer shelf; as a consequence, seasonal variations in the
inshore temperature and salinity are much larger than those offshore. Cross-shelf exchange of
16 water and plankton is effected by (1) large-scale meandering of the Leeuwin Current, (2)
horizontal mixing as tongues of Leeuwin Current water penetrate across the shelf, (3) cascading
18 of high-density coastal water offshore along the seabed, and (4) sporadic summer upwelling onto
the outer shelf (including the wake effect north of Rottnest Island).

20 Nutrient and chlorophyll concentrations are low in comparison with other typical west
coast situations. While there is some indication of a seasonal cycle, the relatively short sampling
22 period and high patchiness have precluded definitive patterns being described and longer-term
sampling may be required to resolve this.

24 The effects of smaller-scale temperature and chlorophyll variability on satellite remote
sensing measurements (both "within-pixel" and "between pixel") in these coastal waters have
26 been quantified using the underway (horizontal) and profile (vertical) data from the surveys. The

project has demonstrated the great potential of using remote sensing information for regular
28 monitoring of the Western Australian continental shelf waters provided that adequate in situ
validation measurements are also undertaken.

30 *Keywords:* hydrography, remote sensing, chlorophyll

1. Introduction

32 Australia possesses an extensive coastline and Exclusive Economic Zone (EEZ) that
covers over 30° of latitude and encompasses tropical, subtropical and temperate realms, giving
34 rise to a great diversity in bioregions. The Australian National Oceans Policy (Environment
Australia, 1998) provides the motivation to understand these bioregions as a precursor to
36 developing management strategies for conservation and utilisation for public and commercial
benefit. The latter include fishing, tourism, recreation, resources development, and maintenance
38 of cultural and heritage values. An integrated, ecosystem-based approach to planning and
management of marine and coastal environments is required and there is significant support for
40 the adoption of a bioregional marine planning approach as the most appropriate strategy.

The Interim Marine and Coastal Regionalisation for Australia (IMCRA) provides the first
42 major attempt at such bioregionalisation at a national level. Briefly, regions were defined at three
spatial scales and based on the available physical and biological data. Sixty diverse meso-scale
44 regions covering the entire coastline and continental shelf were defined and described (IMCRA,
1998), with the metropolitan waters of Perth falling on the boundary between the Central West
46 Coast (CWC 33) and Leeuwin-Naturaliste (LNE 34) regions. The Hillarys Transect is on the
southern limit of the CWC region. However, the available data in most of the remote regions
48 were sparse and varied, indicating that much more data collection and research were required in
order to understand the regional variability in the physical oceanography and the basic
50 biogeochemical processes. The establishment of baseline conditions in a bioregion and the
identification of the natural variability under seasonal and interannual climatic forcing are
52 essential elements in the description and understanding of a bioregion.

It is important therefore to develop and evaluate methods for a systematic study of
54 selected coastal bioregions to support their classification, monitoring and management. Since
satellite remote sensing can play a crucial role in such bioregion monitoring, a number of
56 standard and evolving remotely sensed ocean products should be evaluated to determine their
accuracy and utility in support of bioregion management.

58 This provides the motivation for the present research in Perth's coastal waters, which
have some unique features. Instead of a cool northwards boundary current (as found off the west
60 coasts of southern Africa and South America), the dominant current off Western Australia is the
warm *south*-flowing Leeuwin Current (Godfrey and Ridgway, 1985). The lack of large-scale
62 upwelling (which occurs in the Benguela and Humboldt Current regions) results in a generally
nutrient- and chlorophyll-poor ocean environment (Rochford, 1980; Pearce *et al.*, 2000; Lourey
64 *et al.*, 2006), with the commercial fisheries being dominated by benthic invertebrate species
rather than pelagic fish (Lenanton *et al.*, 1991; Caputi *et al.*, 1996). The major sources of
66 nutrients along the Western Australian continental shelf are river run-off and local inshore
recycling, with only a small contribution from sporadic localised upwelling (Gersbach *et al.*,
68 1999; Hanson 2005a).

Because of the large expanse of the Western Australian coastline, satellite remote sensing
70 provides the only feasible means of monitoring the near-surface water properties along the
continental shelf on a regular basis. Sea-surface temperature (SST) data can show current
72 circulation patterns provided the thermal gradients are sufficiently distinctive, and water
temperature is also an important factor in marine ecology and fisheries. Estimates of the
74 chlorophyll content of the water (and hence phytoplankton abundance and distribution) can be
obtained from ocean colour satellite imagery, although there are potential problems of
76 interpretation near the coast because of non-phytoplanktonic components in the water (so-called
“Case 2” waters), bottom reflection effects and the proximity of land. It is important, therefore,

78 to validate the remotely-sensed data using *in situ* measurements of temperature and chlorophyll
to ensure that the satellite-derived estimates can be applied with confidence in coastal waters.

80 As part of a national program for validation of both SST (NOAA-AVHRR) and ocean
colour (SeaWiFS) satellite imagery, monthly surveys were undertaken on a transect across the
82 continental shelf off Perth in southwestern Australia (Figure 1) between 1996 and 1998. The
surveys were termed the “Hillarys Transects” as they extended due westward from Hillarys
84 Marina (31°50'S). The inshore stations were in the nominally pristine waters of the Marmion
Marine Park (CALM, 1992) while the offshore stations were along the outer continental shelf
86 and hence likely to be influenced by the Leeuwin Current.

To improve our knowledge of the physical and biological processes on the continental
88 shelf off Perth, the opportunity was also taken to monitor a much wider range of physical, optical
and biological quantities than those required simply for satellite validation. With rapid growth in
90 the population of metropolitan Perth (the capital city of Western Australia) and the resulting
pressures on the coastal marine environment, it is increasingly important that the water
92 properties on the continental shelf are well understood. While some major studies have been
undertaken in this region over the years, mainly for effluent dispersal purposes, there have been
94 no systematic surveys examining the physical, biological and optical water properties across the
continental shelf. This project was therefore the first consistent interdisciplinary study of the
96 water across the continental shelf of southwestern Australia.

The objectives of the Hillarys Transect surveys were:

- 98 1) To characterise the physical, chemical, optical and biological properties of the continental
shelf waters off Hillarys (IMCRA region CWC 34) in terms of seasonal and cross-shelf
100 variability;
- 2) To examine relationships between biological distributions and the oceanographic climatology;
- 102 3) To use the *in situ* near-surface observations to validate satellite measurements of water
temperature and ocean colour.

104 4) To assess whether relatively simple in situ measurements complemented by satellite
observations can provide adequate information for defining the dominant characteristics of
106 coastal bioregions.

This paper introduces the transect and measuring techniques, provides some relevant
108 background meteorological and oceanographic information, and presents the results of the
oceanographic measurements (temperature, salinity, nutrients, chlorophyll). It has a dual focus
110 on seasonal relationships across the continental shelf and on the quality of surface measurements
for local validation of remotely sensed data. As such, it also serves as an introduction to the
112 companion papers on bio-optical properties and phytoplankton (Fearnis et al., submitted),
zooplankton (Gaughan et al., submitted) and SST (McAtee et al., this volume), and provides an
114 overview and integration of the salient results from those papers.

The Hillarys Transect surveys complement and extend earlier work on the Perth
116 continental shelf including the Southern Metropolitan Coastal Waters Study (1991 to 1994;
Department of Environmental Protection, 1996) and the Perth Coastal Waters Study (PCWS,
118 also 1991 to 1994; Lord and Hillman, 1995) which examined the assimilative capacity of the
metropolitan coastal waters for increased effluent loadings from submarine outlets. The two
120 outlets nearest to Hillarys are the Ocean Reef and Swanbourne outlets, situated some 7 km north
and 15 km south of Hillarys, respectively (Figure 1).

122 During the PCWS, detailed measurements were made of the ocean currents, water
properties and nutrients (inter alia) near the existing Ocean Reef outlet between December 1992
124 and January 1994, and the results were then integrated into a hydrodynamic/ecological model to
represent the main features of nutrient cycling in the area. The primary focus of the study was
126 the inner continental shelf, although a series of inshore surveys were undertaken across the shelf
some distance north of Hillarys (Pattiaratchi et al., 1995; Zaker et al., submitted). The intensive
128 fieldwork component of the PCWS has given way to an ongoing monitoring project (“Perth
Long-term Ocean Outlet Monitoring” = PLOOM) which has subsequently sampled the water

130 quality in the vicinity of the coastal outlets in the Perth area on a regular basis (e.g. Institute for
Environmental Science, 2002).

132 **2. Climatological and oceanographic background**

2.1. Winds and rainfall

134 The climate and seasonal variability of the mesoscale wind field of the southwestern
coast of Australia are dominated by the meridional shift in the position of the subtropical high-
136 pressure belt. During the southern summer, this belt is at its southernmost limit of about 40°S
(thereby lying south of the Australian landmass; Gentili, 1971) resulting in a net southerly wind
138 system (Figure 2). Strong coastal sea-breezes (particularly during summer afternoons: Masselink
and Pattiaratchi, 2001) are caused by large land-sea temperature contrasts and result in a switch
140 between south-easterlies in the morning and south-westerlies in the afternoon. The afternoon
southerlies continue to dominate into autumn and spring (Figure 2). In winter, on the other hand,
142 the high pressure belt migrates northwards to about 30°S, allowing the eastward passage of
travelling cyclones and storm fronts along the southern and southwestern coasts and resulting in
144 a much more variable wind system with little sea-breeze pattern.

Steedman and Craig (1983) classified the wind systems into 6 main categories with the
146 following speed ranges: land/sea breezes 0 to 15 m/s (spring-to-autumn months), winter high-
pressure systems about 5 m/s (autumn/winter), low-pressure systems 5 to 20 m/s (throughout the
148 year), summer high-low pressure systems about 5 m/s, dissipating tropical cyclones (which
occasionally extend southwards to the latitude of Perth in summer) 10 to 20 m/s, and calms
150 defined as less than 1.5 m/s. Clearly, the coastal winds are highly variable on a range of temporal
and spatial scales as a result of the combination of the geostrophic wind, the land/sea-breeze
152 cycle, storm events and a residual of shorter-term fluctuations (Breckling, 1989).

The only river of note in the Perth metropolitan area is the Swan River some 25 km to the
154 south of the transect. Rainfall in this area is highly seasonal with some 80% of precipitation
occurring between May and October. The monthly median rainfall on the mainland peaks at

156 about 160 mm between June and August (130 mm at Rottnest Island in July), while during the
summer months it falls to < 10 mm (unpublished data, Bureau of Meteorology:
158 <http://www.bom.gov.au/climate/averages/tables>). The response of the Swan River lags by a
month or so, with the highest monthly median discharge of about 60,000 Mlitres in August
160 (unpublished data, courtesy of the Department of Environment); the monthly discharge drops
rapidly after September and is less than about 1000 Mlitres between December and April. The
162 coastal currents tend to flow southwards in winter, and it is only after the seasonal current switch
in September/October (Steedman and Associates, 1981) that riverine outflow could perhaps be
164 carried northwards along the coast by the developing Capes Current.

Evaporation greatly exceeds precipitation between September and April (Bureau of
166 Meteorology, 1966).

2.2. *The Leeuwin Current*

168 The Leeuwin Current is a southward flow of relatively low salinity tropical water along
the Western Australian coast, the only significant poleward eastern boundary current in the
170 world and as such is completely different from the equatorward Benguela and Humboldt
Currents occurring off the west coasts of southern Africa and South America. It is forced by an
172 anomalously large meridional pressure gradient resulting from the throughflow of low-density
equatorial Pacific Ocean water through the Indonesian Archipelago into the tropical eastern
174 Indian Ocean (Godfrey and Ridgway, 1985). The Leeuwin Current flows most strongly during
the autumn and winter months when the alongshore pressure gradient is strongest and the
176 opposing (equatorward) wind stress is weakest (Godfrey and Ridgway, 1985; Smith et al., 1991;
Feng et al., 2003).

178 The presence of the Leeuwin Current is responsible for the occurrence of corals and a
variety of tropical marine organisms and birds much further south than would otherwise be the
180 case (Hutchins, 1991; Hutchins and Pearce, 1994; Dunlop and Wooller, 1990; Maxwell and
Cresswell, 1981; Hatcher, 1991). It is relatively shallow (<300 m) and narrow (50 to 100 km),

182 and tends to flow southwards along the edge of the continental shelf. Periodically, however,
large meanders carry the warm water over 200 km from the shelf (Cresswell, 1980; Pearce and
184 Griffiths, 1991; Department of Environmental Protection, 1996). Woo et al. (2006) suggest that
these meanders may entrain relatively high-chlorophyll shelf waters and transport them into
186 offshore eddies thus effectively exporting chlorophyll from the shelf, while Mills et al. (1996)
found that some shelf-break upwelling can also result from the meandering process.

188 The strongest surface temperature gradients visible in thermal satellite images generally
occur along the offshore (western) boundary of the Current; the gradients along the inshore
190 boundary of the Current are weaker, which can create some difficulty in unambiguously
distinguishing between Leeuwin Current and shelf water regimes (see later). As shown by
192 Cresswell (1996), however, while the strongest currents approaching 1 m/s are generally within
the Current as visible in the satellite images, relatively strong southward currents can still occur
194 beyond the offshore Current “boundary” SST front, raising some questions perhaps of how the
Leeuwin Current is actually defined.

196 As no current measurements were made during the period of the Hillarys Transects, the
historical PCWS current data (Lord and Hillman, 1995; Pattiaratchi et al., 1995) have been re-
198 analysed to summarise the shelf and coastal current regimes. During the PCWS, currents were
measured at two “deep-water” sites near the shelf-break and three “shallow-water” sites along
200 the inner shelf north of the Hillarys Transect between December 1992 and January 1994. The
outer shelf current meters were initially deployed for 4 months (until March 1993) at a site in
202 about 200 m water depth, and the mooring was then moved inshore to a depth of 110 m for the
next 10 months -- for convenience, these two deployments have been simply merged to describe
204 the outer shelf flow over the full year. The monthly mean alongshore current components at
about mid-depth (Figure 3a) illustrate the relatively strong southward currents for most of the
206 year. The strongest currents were in March 1992 where the southward component averaged over
40 cm/s, while individual current speeds in this month were up to 80 cm/s. The relative

208 proportions of the alongshore flow in 90° sectors northward and southward (Figure 3b) confirm
that there was a persistent southwards tendency throughout the year although there were also
210 appreciable periods of northwards flow along the shelf-break for the second half of the
measuring period. More detail of the current measurements can be found in Pattiaratchi et al.
212 (1995), who pointed out that the Leeuwin Current was relatively weak during the PCWS period.

2.3. Shelf currents and the Capes Current

214 The PCWS current measurements on the inner continental shelf showed that the
nearshore waters are largely wind-driven, particularly during the summer months when there is a
216 persistent northwards wind stress (Lord and Hillman, 1995).

As the southerly (northward) wind stress strengthens during the late spring months, the
218 Leeuwin Current tends to weaken and move slightly offshore. A seasonal wind-driven inshore
countercurrent (the Capes Current -- Pearce and Pattiaratchi, 1999; Gersbach et al., 1999;
220 Cresswell and Griffin, 2004) forms near or south of Cape Leeuwin some 250 km south of Perth,
associated with localised upwelling between Cape Leeuwin and Cape Naturaliste and forming
222 the main source of the Current (Gersbach et al., 1999; Hanson et al., 2005a). The Capes Current
transports relatively cool water northward past Rottnest Island between October and March, and
224 Woo et al. (2006) found evidence of Capes Current water as far north as Shark Bay (26°S).
During the remainder of the year, the mid-shelf currents tend to flow southwards but with many
226 weather-related reversals (Steedman and Associates, 1981; Cresswell et al., 1989; Pattiaratchi et
al., 1995).

228 A re-analysis of the PCWS current measurements was undertaken for the mooring site
SW2 (water depth 27 m about 8 km offshore), and showed a far more distinct seasonal pattern
230 than at the shelf break. The northwards Capes Current was the dominant flow during the summer
months of October to February, illustrated by both the mean alongshore component (Figure 3c)
232 and the relative frequency of the northwards currents over that period (Figure 3d). In winter
when the Capes Current had ceased, there was a small net southwards tendency but the current

234 directional frequencies nevertheless showed a good proportion of northward flow as well. Peak
near-surface current speeds sometimes exceeded 50 cm/s but were more commonly about 30
236 cm/s. These results effectively matched some earlier measurements made in 20 m water depth 4
km west of Point Peron just south of Perth (Steedman and Associates, 1981) which showed a
238 very distinct switch between northwards currents from October to April and a net southwards
flow between May and September.

240 Subsequent oceanographic surveys around Rottnest Island in 1995 combined with
satellite imagery revealed that a cool plume extending northwards in the wake of Rottnest Island
242 during the summer months resulted from a secondary circulation induced by curvature of the
Capes Current past the offshore tip of the Island (Alaee, 1998; Alaee et al., 1998). The cooler
244 water was drawn up from the outer shelf just west (offshore) of the Island creating a dome of
upwelled water on the mid-shelf north of the Island. (As will be shown below, this has an
246 important effect on the water structure along the Hillarys Transect).

Despite the dominance of the wind stress in forcing the nearshore flow, Zaker et al.
248 (submitted) found that, on occasion, meanders of the Leeuwin Current onto the shelf had a direct
influence on the currents nearer the coast. Similarly, Mills et al. (1996) observed that a
250 northwesterly wind in winter 1991 led to an onshore surface migration of warm Leeuwin Current
water accompanied by downwelling and an active flushing of the inner shelf by offshore
252 transport near the seabed. Under weaker wind conditions, a mesoscale anti-cyclonic meander of
the Leeuwin Current forced a northward flow along the shelf and some upwelling.

254 The tidal regime along the southwestern coast is predominantly diurnal, and because of
the small tidal range (up to 0.6 m), tidal currents in the area are negligible.

256 **3. Data and Methods**

3.1. The Transect

258 The transect consisted of 9 stations H0 to H40 (Figure 1, Table 1) extending to 40 km
offshore (the numerical suffix denoting the station distance from the coast in km). The latitude

260 was selected to ensure safe passage through a gap in the nearshore reef system some 4 km
offshore. From the reef, the seabed slopes down to station H5 beyond which lies a gentle plain
262 some 30 to 45 m deep before the seabed finally drops away suddenly at an escarpment some 37
km offshore (Figure 4). Station H0 was in the nearshore lagoon, and all the stations except for
264 H40 were in water less than 50 m deep. The only bathymetric feature likely to influence the shelf
circulation was the nearshore reef system which could tend to channel the alongshore flow at the
266 innermost station. Station positions were fixed by the vessel's GPS.

A total of 27 monthly transects were undertaken between October 1996 and December
268 1998. However, methods were still being developed and equipment evaluated during the first 3
surveys, so some of the results are presented for only part of the 27 month period.

270 On the outward (westward) leg of each transect, both surface and profile measurements
were taken at each station; the homeward leg was a continuous run, except for (from March
272 1997) a repeat stop at H5 for a comparison of the morning and afternoon conditions. Throughout
each trip, surface temperature, conductivity and fluorescence were recorded continuously. The
274 round trip typically took about 5 hours, departing the quayside at 0900 WAST (Western
Australian Standard Time). The arrival of the seabreeze around midday usually raised sea
276 conditions at the outer Transect stations, with winds frequently exceeding 10 m/s (Masselink &
Pattiaratchi, 2001), but such conditions were in fact beneficial for the SST validation work by
278 ensuring vertical mixing down the upper water column.

The schedule covered the pass of the SeaWiFS satellite, while the afternoon NOAA-14
280 pass was generally within a couple of hours of the end of the transect. While attempts were made
to run the surveys on days when the sea was reasonably calm and the skies clear (for the satellite
282 validation), personnel and boat commitments necessitated occasional trips in adverse or cloudy
conditions. On only one occasion (August 1998) did weather conditions prevent the complete
284 transect to H40 being completed.

3.2. *Meteorology*

286 Some simple wind measurements were made using a hand-held anemometer from the
bow of the boat at each station to provide an indication of “on-station” winds. Although hourly
288 meteorological data were available from a weather station in Hillarys Marina operated by the
National Tidal Centre, the measurements are considered unrepresentative of the coastal waters
290 because of the low height of the anemometer and some “sheltering” from adjacent buildings.
Accordingly, wind data were obtained from an Automatic Weather Station (AWS) operated by
292 the Australian Bureau of Meteorology at Rottnest Island (Figure 1); the base of the AWS is 43 m
above mean sea level, and the anemometer is 10 m above ground level. (The Rottnest wind
294 speeds were more than double those from the Hillarys anemometer).

Wet- and dry-bulb air temperatures were measured on station using a hand-held sling
296 psychrometer.

3.3. Underway measurements

298 “Surface” temperature was logged continuously from a through-flow system drawing
water from a depth of about 50 cm, together with time and GPS position; the specified accuracy
300 of the temperature sensor was ± 0.1 °C. Fluorescence was measured simultaneously during the
1998 surveys using a Wetstar fluorometer, calibrated against chlorophyll concentration using
302 water samples drawn at regular intervals from the flow system. The temperature and
fluorescence were recorded on a laptop computer initially at 5-second intervals, representing an
304 along-track sample about every 40 m at the cruising boat speed of 16 knots or 8 m/s, and later at
2-second intervals. We estimate that the time for the water to flow through to the sensors was
306 about 5 seconds, during which time the vessel would have moved through about 40 m which is
unimportant for our purposes.

3.4. On-station measurements

At each station, vertical temperature/conductivity profiles were obtained using a Yeokal
310 Model 606 Submersible Data Logger (SDL; rated temperature accuracy ± 0.1 °C, resolution 0.01
°C) sampling at 1 second intervals. Unfortunately, the conductivity sensor on the SDL proved

312 unreliable and so the subsurface salinities are not discussed in any detail in this paper. The
instrument was lowered into the water from the bow of the vessel and held within the top 50 cm
314 for about a minute to stabilise the sensors and provide good "surface" data. It was then lowered
by hand at a speed of about 1 m/s to touch the seabed at all stations (except H40 where the depth
316 was too great), and raised again to the surface, where it was held at the surface for another
minute before being brought back on board. During the first two transects, profiles were only
318 taken at stations H0, H10, H20, H30 and H40. The SDL failed in February, July, August and
September 1998. 1-m depth-averages were computed for each down- and up-cast.

320 As an independent near-surface temperature measurement, "bucket" samples were taken
using a 15-litre plastic bucket scooping water from the top 30 cm or so, some distance away
322 from the engine cooling-water outlets. The bucket was brought on deck into the shade and the
temperature noted immediately using a mercury thermometer graduated to 0.1 °C. The mercury
324 thermometers were calibrated in a laboratory tank against reference thermometers reading to
0.01 °C; the estimated accuracy of the bucket temperatures was ± 0.1 °C, with perhaps a similar
326 "error" resulting from possible temperature changes within the bucket between taking the sample
and reading the temperatures. This accuracy was adequate for our purposes, and there was a
328 good correlation (0.99) between the surface temperatures measured using the bucket, the SDL
and the underway sensor. A salinity sample was also taken from the bucket and later analysed in
330 the shore laboratory using an Autolab salinometer, with a rated accuracy of ± 0.003 psu.

For the satellite SST validation, some extra measurements were made of the temperature
332 within a few cm of the water surface using a floating thermister while the "skin" temperature was
measured with a TASCOR radiometer (see McAtee *et al.*, this volume).

334 3.5. Nutrient and chlorophyll samples

On each station, vertically-integrated water samples were obtained by pumping water
336 through a hose which was lowered from the surface to a depth of 18 m (or near the bottom in
shallower water) and back to the surface. Chlorophyll samples were collected by filtering 5 litre

338 volumes through Whatman GF/C filters (47mm diameter), which were stored in the dark in
plastic centrifuge tubes on ice. Back at the laboratory, the filter was placed in a 10 ml test-tube
340 and 8 ml of a 90:10 (vol:vol) acetone:water solution were added. The sample was then sonicated
for 10 minutes in an ultrasonic bath to break down the cells, and stored at 4°C overnight. The
342 sample was filtered again through a GF/C filter into a clean 10 ml test-tube.

These samples were analysed using both a Varian DMS-90 UV/VIS spectrophotometer
344 and a Turner fluorometer. A 90:10 acetone:water solution was initially used in both the reference
and sample cuvettes on the spectrophotometer; the absorbance was read and the machine zeroed
346 at each wavelength (480, 510, 630, 647, 664 and 750 nm). Each chlorophyll sample was then
inserted into the sample cuvette in the spectrophotometer and the absorbance read at each
348 wavelength. Periodically (after 10 to 15 samples), the acetone sample was again placed in the
sample cuvette and the "blank" reading noted. After the spectrophotometer analyses, the test-tube
350 samples were also analysed for fluorescence using a Turner Fluorometer following the
acidification technique of Parsons et al. (1989).

352 Replicate nutrient samples were taken at each station; these were frozen and stored for
subsequent analysis in the shore laboratory for nitrate, silicate and phosphate concentrations
354 using standard analytical methods (Cowley et al., 1999). As the nutrient samples prior to
September 1997 were unfortunately lost due to handling/contamination errors, only the results
356 after this date are presented here.

3.6. Optical measurements

358 As part of the validation of ocean colour from SeaWiFS, optical measurements were
taken on each station. Simple Secchi depths were derived by observing the depths at which the
360 disc was just no longer visible (down-cast) and when it first became visible again on the up-cast;
there was some subjectivity in this measurement depending on the skill and experience of the
362 operators and on factors such as sun-glint, shading by the vessel and surface roughness.
Subsurface light profiles were obtained using a 4-PI Li-cor LI-250 Lightmeter, giving an

364 estimate of the reduction of Photosynthetic Available Radiation (PAR) with depth. This part of
the study is dealt with by Fearn et al. (submitted).

366 3.7. Satellite images

Advanced Very High Resolution Radiometer (AVHRR) satellite imagery has been
368 received in Perth since 1981, and NOAA-14 images for each Hillarys transect date were obtained
from the Western Australian Satellite Technology and Applications Consortium (WASTAC).
370 Full-resolution (1.1 km) images for the region 30° to 35°S were processed to show thermal
structures associated with the Leeuwin Current and coastal waters in the vicinity of the transect,
372 and hence aid interpretation of the transect data. On 6 of the 27 transect days, cloud covered the
transect area so imagery on adjacent days was used if they were cloud-free.

374 Surface temperatures were derived from the brightness temperatures in AVHRR bands 4
and 5 using the McMillin and Crosby (1984) algorithm and also the MultiChannel SST
376 (MCSST) algorithm, the coefficients for which were obtained from the NOAA website
<http://www.osdpd.noaa.gov/EBB/pubs/SST/noaa14sst.asc>. The two algorithms are compared
378 against the surface radiometer temperatures in the companion paper by McAtee *et al.* (this
volume). Digital SST transects extending much further offshore than the Hillarys stations were
380 extracted from the AVHRR data to complement the transect temperature measurements by
providing a larger-scale perspective on the surface thermal structure and position of the Leeuwin
382 Current in relation to the shelf waters and the transect stations.

SeaWiFS chlorophyll images were obtained from WASTAC after the satellite was
384 launched in December 1997. Chlorophyll concentrations were derived using SeaDAS software
supplied by NASA; relationships between the *in situ* chlorophyll measurements and the satellite
386 data are dealt with in the companion paper by Fearn et al. (submitted).

4. Results and Discussion

388 In this section, we present the main oceanographic results from the Hillarys Transects,
focusing on the seasonality and cross-shelf variability of temperature, salinity, chlorophyll and

390 nutrients. In addition, some estimates are made of uncertainties in the validation of satellite-
derived SSTs and chlorophylls as a result of the observed small-scale horizontal and vertical
392 gradients.

4.1 Meteorology

394 The meteorological measurements from Rottneest Island during the period covering the
Hillarys Transects effectively match the seasonal wind roses of Figure 2. The wind vectors show
396 that the winds were dominantly from the southerly sectors between about October to March
(Figure 5), but were much more variable in winter and had a net north-westerly tendency. The
398 wind stability, which is defined as the ratio of the vector wind speed to the scalar wind speed
(Neumann, 1968) and is an indication of the persistence of the wind in any particular sector,
400 showed a corresponding strong seasonality with values of over 70% during the persistently
southerly winds in summer and as low as 10% in winter (Figure 5).

402 Monthly mean scalar wind speeds (derived as the simple averages of the hourly wind
speeds) varied between 6 and 9 m/s, but the hourly speeds often exceeded 20 m/s and peak
404 individual gusts during the late autumn/winter months approached 30 m/s (almost 60 knots).

4.2 Satellite imagery and the Leeuwin Current

406 An overall perspective on the dominant seasonal circulation patterns across the shelf and
further offshore can be gained from the satellite thermal images and digital transects. In general,
408 the Leeuwin Current tended to flow along the shelfbreak or further offshore (Smith et al., 1991),
sometimes in the form of a large anticyclonic meander (Pearce and Griffiths, 1991). While its
410 full strength (associated with the warmest water and the strongest SST gradient) generally
occurred beyond the shelfbreak, the Current was also observed to spread onto the outer shelf and
412 indeed at times appeared to be fully contained on the shelf (as in Cresswell, 1996) -- on such
occasions, it was encountered towards the offshore end of the Transect.

414 The winter situation may be typified by the SST image in July 1997 (lower panel in
Figure 6), showing the warm Leeuwin Current flowing southwards as a narrow, well-defined

416 stream slightly overlapping the Transect on the outer continental shelf, with some offshore re-
circulation in the form of a cyclonic eddy. Just to the north was the zonal southern boundary of a
418 strong anticyclonic meander, the shorewards flow evident in the small cyclonic shear eddies
along the Current boundary. The corresponding digital SST transect (Figure 7, lower curve)
420 clearly showed the southflowing current and the warm northward eddy flow (separated by the
cool eddy core) and beyond this the temperature dropped by over 3°C in a series of steps to the
422 open-ocean water west of 114°E. The nearshore water was 2°C cooler than the Leeuwin Current,
and the Transect SDL stations closely matched the cross-Transect gradient in the AVHRR
424 profile.

In January 1997, by contrast, the Leeuwin Current was further offshore and well beyond
426 Transect station H40 (upper curve in Figure 7); the cooler Capes Current was flowing
northwards along the mid- and outer shelf regions, and a band of warmer summer-heated water
428 hugged the coast. This nearshore band was now 2 °C warmer than the Capes Current, again well
matched by the satellite profile, and the thermal relief across the Leeuwin Current was about 1
430 °C. Figures 6 and 7 well demonstrate the value of using satellite imagery to provide a larger-
scale perspective to localised surveys.

432 In many of the satellite images (particularly in the winter/early spring months when the
thermal contrast between the coastal and offshore waters was greatest), cross-shelf
434 advective/mixing events were evident as tongues of Leeuwin Current water penetrating onto and
across the continental shelf (Pearce and Griffiths, 1991). They could be broad (of order shelf
436 width) and weakly-defined areas of warm water spreading right across the shelf apparently to the
coast, but at other times they were much narrower (and presumably stronger) jet-like flows,
438 representing an exchange of heat/salt between nearshore and offshore waters and thus providing
an active mechanism for the exchange of planktonic larvae across the shelf. As an example, in
440 July 1997 the Leeuwin Current “wrapped-round” the southern coast of Rottnest Island (Figure 6,
lower panel); this form of intrusion helps explain the presence of reef-building corals and the

442 annual settlement of larval tropical fish along the south coast of the Island (Hutchins and Pearce,
1994; Hutchins, 1999).

444 On the other hand, in October of both 1997 and 1998 (the latter shown in the lower panel
of Figure 8), an intrusion was curving in towards Rottnest Island from the north -- a remarkably
446 similar pattern was observed using Landsat imagery in August 1991 (Wyllie et al., 1992;
Department of Environmental Protection, 1996; Mills et al., 1996) and showed the interaction
448 between the Leeuwin Current and a plume of discoloured water from the Peel-Harvey estuary
well south of Perth.

450 These cross-shelf mixing events have been observed elsewhere along the Western
Australian coast (see satellite images in Legeckis and Cresswell, 1981; Pearce and Griffiths,
452 1991; Pearce, 1997). A re-analysis of historical current meter records near the Houtman
Abrolhos Islands (29°S; Cresswell et al., 1989) by Pearce and Phillips (1994) showed that cross-
454 shelf current speeds were typically up to 10 cm/s and could persist for a few days. Since 1 cm/s
~~ 1 km/day, planktonic larvae can be passively transported cross the 40 km wide shelf (either
456 towards or away from the coast) within a week, while actively-swimming animals such as the
puerulus stage of the western rock lobster would be greatly assisted (or hindered) by cross-shelf
458 currents (Pearce and Phillips, 1994; Griffin et al., 2001). The re-analysis of PCWS current
measurements mentioned earlier showed that there was little seasonality in the cross-shelf flow;
460 currents at the 27m site were either onshore or offshore (with no preference) for between 10 and
25% of the time in any month of the year. (Onshore currents were defined as being in the sectors
462 between NE and SE, and offshore flow was between NW and SW).

The satellite images also frequently showed an upwelling plume north of Rottnest Island
464 during the summer months (as in January 1998, Figure 8 upper panel), associated with a
secondary circulation due to the curvature of the flow around the western tip of the Island when
466 the Capes Current was flowing (Alaee, 1998; Alaee et al., 1998). While the northward extent of

the plume in the satellite images was usually restricted to 2 or 3 island widths (but still crossed
468 the Hillarys Transect), on at least one occasion it seemed to extend far beyond that.

4.3. *Surface temperature and salinity*

470 The surface temperatures at the Transect stations showed a marked seasonal reversal of
gradient across the continental shelf (Figure 9a), resulting in a change of both amplitude and
472 phase in the annual temperature cycle between the inshore and offshore waters. At station H0
close inshore, water temperatures peaked at 22 to 23°C in January and dropped to 16° in June
474 1998 (July/August in 1997), giving an annual temperature range of 7°C near the coast. In the
deeper offshore waters, on the other hand, where the influence of the Leeuwin Current was more
476 apparent, the temperature rose from 21°C in January to 23°C in April/May 1998 before falling
gradually to a trough of 20°C in September -- an annual range of only 3°C. The cross-shelf
478 temperature differential accordingly reversed from -1°C in January to +6°C in June;
February/March and December were transition months when the cross-shelf gradients were
480 minimal. The warmest water (24.1°C) was observed at H0 in January 1997 and the coolest
(15.9°C) again at H0 in June 1998. Summer temperatures near the coast were higher in 1997
482 than in 1998, while those at the shelf break were higher in 1998 than in the previous year;
however, no realistic interannual pattern can be deduced from just these two years.

484 The salinity transects (Figure 9b) presented a similar picture albeit less clearly defined,
with most of the variability again occurring near the coast. Inshore surface salinities were well
486 above 36 psu in summer (exceeding 36.6 psu in February 1997) as a result of evaporation (Zaker
et al., submitted); monthly evaporation at Perth exceeds 250 mm in mid-summer (Bureau of
488 Meteorology, 1966), and this high-salinity water extended as far offshore as station H20 in 1997
and H15 in 1998. The salinity then fell rapidly as the winter rainfall commenced in May and
490 low-salinity Leeuwin Current water mixed onto the shelf. By mid-year, the salinity was fairly
uniform at about 35.5 psu across the shelf and there were pulses of <35.4 psu water close inshore

492 in late winter. At the offshore station H40, summer and winter salinities were respectively about
36 and 35.5 psu giving a seasonal variation of only 0.5 psu compared with 1.1 psu close inshore.

494 The lowest surface salinities recorded during the surveys were 35.0 psu at the nearshore
station H0 in September 1997, 35.24 psu at the same station in November 1998, and 35.26 psu at
496 H5 (not H0) in September 1998 (Figure 9b). In the September 1997 survey, the low salinity
water at H0 extended down to the seabed (water depth of only 6 m); the surface and bottom
498 salinities at H5 were about 35.4 and 35.6 psu respectively with a very strong halocline at mid-
depth while the salinities from H10 outwards were all above 35.65 psu, suggesting a local
500 inshore source of the fresh water which then extended offshore as a surface lens over more saline
water at H5. The wind speed was only about 2 m/s at the inshore stations.

502 Monthly mean temperatures and salinities have been derived from the full 27-month
period for stations H0 and H5 (representing inshore waters) and H35-H40 (outer shelf) to
504 summarise the annual surface temperature and salinity cycles (Figure 10) across the shelf.
Effectively, the shallow inshore waters are largely influenced by air-sea heat fluxes and by
506 rainfall/runoff and evaporative processes while the Leeuwin Current plays the dominant role
along the outer shelf.

508 Approximate limits can be assigned to the water properties for the inner and outer shelf
using the surface T/S characteristics (Figure 11) for the two innermost and two outermost
510 stations:

	Inner shelf (H0/H5)	Outer shelf (H35/H40)
512 Summer	$T > 21^{\circ}\text{C} / S > 36.0 \text{ psu}$	$21^{\circ} < T < 23^{\circ}\text{C} / 35.7 < S < 36.0 \text{ psu}$
Winter	$T < 18^{\circ}\text{C} / S < 35.6 \text{ psu}$	$19^{\circ} < T < 21^{\circ}\text{C} / 35.4 < S < 35.6 \text{ psu}$

514 As is shown below, vertical mixing generally ensures that the deeper shelf water
properties are little different from those at the surface.

516 Although there are no river outflows in the immediate vicinity of the Hillarys Marina
(and no freshwater discharges into the Marina), effluent plumes from the Swan River some 25

518 km to the south (Figure 1) could perhaps extend northwards along the inner- to midshelf when
the coastal currents reverse to northgoing in September (Steedman and Associates, 1981; Zaker
520 et al., submitted). As mentioned in Section 2.1, the peak monthly river discharge occurs in
August and there is still a substantial outflow in September after which the flow is generally an
522 order of magnitude lower. Sampling by Gaughan and Potter (1994) just inside the river mouth
showed that surface salinities can be as low as 12 psu in August.

524 There appear to be no published salinity measurements along the shelf north of the Swan
River of sufficient spatial and temporal resolution to show any freshwater influence from the
526 river, but Mills et al. (1996) presented a Landsat image revealing a plume of coloured water from
the river mouth extending northward well past the Hillarys region in August 1991.

528 Assuming salinity to be a conservative property, we have used two (unpublished) surveys
of the salinity between the river mouth and Hillarys to examine in more detail the northwards
530 extent of Swan River outflow. The alongshore distribution of salinity at 6 stations between the
Swan River mouth and Scarborough (just north of the Swanbourne ocean outlet -- Figure 1) was
532 measured during 31 surveys between 1985 and 1989 (CSIRO unpublished data: Figure 12). The
lowest salinities recorded just outside the river mouth (station A) were 24 to 26 psu in August
534 (with nitrate concentrations of 8 μM), and depressed salinities (< 35 psu) were occasionally
observed during the winter months within about 5 km of the river mouth at stations V and W
536 (Figure 12). However, these extremes reverted to near-normal coastal values north of this
location (i.e. from station U northwards): monthly mean salinities in winter/spring at stations S,
538 T and U (Figure 1) varied between 35.15 and 35.48 psu and the minimum salinities measured at
those stations were down to 35.0 psu -- very similar to the Hillarys Transect (inshore) means and
540 minima in Figure 10b.

Salinity measurements were also made during the PLOOM monitoring study near the
542 Swanbourne ocean outlet (Figure 1) between 2000 and 2005 (unpublished data, Water
Corporation), with 4 routine sampling stations numbered SB1 (4 km south of the outlet) to SB4

544 (8 km north of the outlet). The sampling programme found that the wastewater plume from the
outlet was generally undetectable more than about 4 km from the discharge point (Institute for
546 Environmental Science, 2002). We have analysed the salinity data from the southernmost and
northernmost stations SB1 and SB4 as least likely to be affected by the freshwater discharge
548 from the outlet. The monthly mean salinities varied between 35.00 and 35.45 psu during the
winter/early spring months while the monthly minima were just below 35 psu -- although these
550 measurements were from close inshore, they were similar to the Hillarys Transect values for
H0/H5.

552 From both studies, it appears that from Swanbourne northwards the winter/spring
salinities are generally not very different from those measured on the Hillarys Transect and it is
554 therefore debatable whether Swan River discharge on a regular basis penetrates as far as Hillarys
without substantial dilution. It is nevertheless possible that on occasion (such as after
556 exceptionally heavy rainfall and strong northwards currents) the river plume could be evident
north of Hillarys (as observed in the published satellite image).

558 Another potential source of freshwater is submarine groundwater discharge (SGD) which
contributes high-nutrient low-salinity water into the nearshore region of Marmion Lagoon
560 (Johannes, 1980; Johannes and Hearn, 1985). Zaker et al. (submitted) have also suggested that
SGD can play an important role in nearshore salinity variability especially during winter.
562 Johannes and Hearn (1985) measured nitrate concentrations of 400 μM in the freshest parts of
the discharge immediately off the beach, and found that reduced salinities (and correspondingly
564 enhance nitrate concentrations) could extend out to 1.5 km from the shore under very calm
conditions although more generally the affected area was less than 300 m offshore. Station H0
566 was within about 100 m of the Marina breakwater, and it is therefore likely that SGD was
responsible for the reduced salinities at that station.

568 *4.4. Water masses*

As shown by Cresswell and Peterson (1993), the Leeuwin Current is a mixture of low-
570 salinity tropical water (brought down from the north) and more saline subtropical water (in the
geostrophic inflow from the west), the latter dominating during the summer months when the net
572 equatorward wind stress reduces the south-flowing tropical component. The Capes Current and
its associated upwelling in the Capes region are also effectively derived from the Leeuwin
574 Current (Gersbach et al., 1999).

High-salinity South Indian Central Water (Rochford, 1969; Cresswell, 1991), which may
576 perhaps be linked with the geostrophic inflow, has previously been identified (by its salinity of
>35.8 psu) intruding from the west along the upper slope near Cape Leeuwin (34.5°S; Cresswell
578 and Griffin, 2004), off Perth (Greig, 1986; Cresswell and Griffin, 2004) and at Geraldton (29°S;
Pearce et al., 1992). Between October and April, the Hillarys outer station H40 frequently
580 encountered subsurface intrusions of more saline water near the seabed with T/S properties of
19° to 22°C and >35.8 psu, indicating the presence of this water mass but it was not observed to
582 penetrate any further onto the shelf. While it is likely that sporadic localised upwelling onto the
outer shelf (as found off the Capes area by Gersbach et al., 1999) is of Central Water origin, the
584 elevated nearshore salinities of 36 to 36.5 psu observed during the summer months are much
higher than those in the Central Water mass and must therefore be a result of evaporation in the
586 shallow water.

As no other "new" water comes into the system, the water on the southwest Australian
588 continental shelf must ultimately be derived from the Leeuwin Current, albeit modified by air-
sea heat and moisture flux and mixing as it moves onto and across the shelf, possibly with some
590 subsurface inclusion of more saline Central Water along the outer shelf and in localised
upwelling on occasion.

To assist interpretation of the physical, nutrient and optical properties as well as the
plankton distributions over the 27-month period, the satellite images have been used in
594 conjunction with the temperature/salinity data to classify the water regime at each station

position (Table 2). Coastal Water (CW) was by definition the water regime at stations H0 and H5
596 within the coastal boundary layer described earlier but at times seemed to extend out to H20 or
even H25. Where the Leeuwin Current could be reasonably identified by its thermal signature
598 the station was classified as LC, but on many occasions the water seemed to be derived from (but
not implicitly part of) the Leeuwin Current and so was labelled Leeuwin Current Water (LCW).
600 Capes Current water (CC) was clearly in the cool band of midshelf water apparently moving
northwards (an exclusively summer phenomenon) and was sometimes evident out to station H40,
602 perhaps more as an absence of the Leeuwin Current rather than a very clear Capes Current itself.
Although the upwelled plume of cooler water north of Rottnest Island is closely linked with the
604 Capes Current, the water in the plume was classified as UW where it could be unambiguously
identified as such. While these distributions are somewhat subjective, the seasonal and cross-
606 shelf patterns were reasonably clear.

These results effectively confirm Zaker et al.'s (submitted) suggestion of a coastal
608 boundary layer of order 10 km wide, although the satellite imagery suggests that this "coastal
water" on occasion extended beyond station H10 (Table 2). The horizontal gradients of
610 temperature, salinity and nutrients between each pair of stations over the 27 months clearly
indicate that most of the hydrographic variability was contained within the coastal band out to
612 station H15 (and the largest gradients were within 5 km of the coast). The nearshore shallow reef
system is an obvious explanation for the changes between H0 and H5, but there are no prominent
614 bathymetric features beyond that as the seabed is a relatively flat plain out to almost H40 (Figure
4). While the Leeuwin Current was identified along the outer shelf on 7 occasions out of 25
616 cloud-free images (with a further 2 possible occurrences, all between March and September --
Table 2), water derived from the Current and mixing onto/across the shelf could be present at
618 any time of year. It penetrated across the shelf on occasion as close inshore as H20 and (rarely)
H15 (Table 2).

620 In summary, the external water masses influencing our continental shelf are the tropical
and subtropical waters of the Leeuwin Current and a summer subsurface intrusion of more saline
622 South Indian Central Water which may on occasion upwell onto the outer continental shelf.
These are then modified by mixing and by air-sea exchange processes as they cross the shelf to
624 form the nearshore waters.

4.5. Vertical structure

626 Apart from the horizontal temperature and salinity variability described above, there were
also changes in the water column structure which illustrate some of the dynamics and are also
628 important for satellite SST validation.

As the conductivity profiles from the SDL proved somewhat unreliable, they are used
630 here only to help explain some of the features of the vertical structure (the salinity changes were
generally small in comparison with those of temperature). Because the SDL was lowered right
632 down to touch the seabed at each station, it was able to sample the bottom mixed layer which
would be unwise with more expensive CTD equipment.

634 The basic temperature structure across the shelf was vertically well-mixed but with the
seasonally-reversing horizontal structure described above. However, vertical stratification was
636 observed irregularly at different stations and in different months through the year, either induced
by surface heating or by the upwelling-like process in the lee of Rottnest Island (described
638 earlier) -- these were both largely summer phenomena.

Particularly in summer, virtually isothermal conditions could prevail right across the
640 continental shelf (e.g. December 1996, Figure 13a), with a narrow band of warmer water within
5 km of the coast and only marginal surface heating. In December 1998 (Figure 13b), by
642 contrast, surface heating resulted in a temperature differential of over 1.5 °C between the surface
and 20 m depth. The strongest stratification was observed at the mid-shelf stations resulting from
644 the Rottnest Island wake upwelling (as in January 1998, Figure 13c) described earlier. The
central plume of the upwelling generally tended to lie near stations H20 to H25 due north of the

646 Island leading to the "doming" evident in Figure 13c. The depth of the dome was typically below
20 m, and as our depth-integrated nutrient sampling extended down to only 18 m depth it was
648 unable to show any nutrient enrichment in the upwelled water mass (Alaee et al. (1998) did not
report on salinity or nutrient measurements in the upwelled plume).

650 The water column was also typically well-mixed during the winter months, but there was
almost invariably a pronounced cross-shelf temperature gradient sometimes intensifying into
652 discrete frontal zones as in June 1998 (Figure 13d). Starting from the coast, there was a rapid rise
in water temperature as a result of heat loss to the atmosphere from the shallow water
654 (Pattiaratchi et al., 1995; Zaker et al., submitted), then a strong mid-shelf front of more than 1.5
°C. The sloping front was fairly common in autumn and winter, probably associated with the
656 downwelling process described by Mills et al. (1996); Symonds and Gardiner-Garden (1994)
have shown that transient downwelling events and weak cross-shelf currents can result from
658 convective cooling of nearshore waters during the winter.

A similar situation was observed during the summer/autumn months when high-salinity
660 nearshore water was denser than the offshore waters despite the coastal warming. In March 1997
for example (not shown here), the temperature, salinity and density of the water at the coastal
662 station H0 were greater than the near-surface waters further offshore but effectively matched the
properties of the near-bottom shelf water.

664 It appears that an intermittent "slumping" or cascading of high-density coastal water
down and across the shelf may occur at any time of year, this downwelling process representing
666 an active mechanism for cross-shelf water and larval exchange (Symonds and Gardiner-Garden,
1994; Wells and Sherman, 2001; Shapiro et al., 2003).

668 The surface mixed layer depth (SMLD) is usually defined either by a specified
temperature (or density) difference from the surface value or by a change in the temperature (or
670 density) gradient. Different temperature departures from the surface value have been used by
various authors: Colborn (1975; 1°C), Longhurst (1995; 0.5°C), Hamilton (1986; 0.2°C),

672 Rochford et al. (2000; 0.1°C), Feng et al. (2003; 0.5°C) and Lourey et al. (2006; 0.4°C from the
10 m temperature), while different thermocline gradients have been defined by other authors:
674 0.05°C/m (Watts and Owens, 1999; Qu, 2001) or 0.5°C/m (Gray and Kingsford, 2003).

We prefer the gradient definition for our shallow water work because use of any specified
676 temperature difference will give a SMLD even if the temperature simply decreases uniformly
with depth and no abrupt change of gradient is actually present. For our purposes, the 1-m depth-
678 averaged temperature profiles were smoothed by a simple 5-point running mean, starting at a
depth of 5 m below the surface to avoid the highly variable near-surface layer. By examining the
680 temperature profiles over the 2-year period, a thermocline was defined as a region in which the
vertical temperature gradient exceeded 0.02 °C/m over at least 5 m depth interval (i.e. > 0.1 °C
682 over the 5 m). Smaller regions (< 5 m) of higher gradients within a mixed layer were thus
effectively ignored as being (for practical purposes) inconsequential. The SMLD was then
684 derived as the water column down to the first thermocline, and the bottom mixed layer depth
(BMLD) correspondingly as the water column from the seabed up to the base of the deepest
686 thermocline.

Using these criteria, the surface mixed layer depth (SMLD) extended throughout the
688 water column to the seabed on 42% of stations, with a weak seasonality. As would be expected,
the shallowest stations were most frequently isothermal, and only at H40 was it a rare occurrence
690 (because of the greater water depth) but even there conditions were effectively isothermal on 4
days out of 22. The SMLD right across the shelf tended to be least during the summer months
692 when the thermocline was up to the water surface. In deeper off-shelf waters, Hamilton (1986)
and Feng et al. (2003) also concluded that the deepest mixed layers occurred during the winter
694 months.

When it existed, the thermocline was typically thin and relatively weak with temperature
696 differences of less than 1 °C across 5 m or more. On only 1 day (January 1998 -- Figure 13c) did
the temperature differential across the thermocline exceed 2 °C. Below the thermocline there was

698 usually a well-defined BML, particularly in the mid-shelf region where the upwelling was
occurring.

700 Near-surface temperature gradients are important for validation studies for satellite-
derived temperatures. Conventionally, validation of satellite SSTs is undertaken using “bulk”
702 temperature measurements from sensors in the upper 1 m or so of the water column whereas the
upwelling radiance sensed by the satellite is actually from a very thin surface “skin” (less than a
704 millimetre in thickness). The temperature difference between the surface skin and the subsurface
layer is typically of order 0.3°C (Robinson et al. 1984) and so very accurate measurements of
706 both are required. The bulk temperature measurements in this study were made using the surface
bucket and the SDL profiler while the “skin” temperature was measured using a radiometer (see
708 McAtee et al., this volume). Neither of these have provided temperatures of sufficient resolution
to address the skin-bulk temperature question, so the SDL profiles (which have a resolution of
710 0.01 °C) are used here to examine the bulk near-surface gradients.

Because of the rolling motion of the vessel while on station, the SDL was moving
712 vertically up and down through the uppermost 1 m or so of the water for the first part of the cast
prior to being lowered through the water column (see Methods). During that time, it was in some
714 sense "profiling" that near-surface layer, and we have taken the highest temperature sampled as
representing the water immediately below the surface skin. Over the 27-month period, the
716 differential between the highest SDL temperature and the 1-m average was less than 0.1°C for
89% of the time and less than 0.2°C for 94%; the maximum value was 0.56°C. This effectively
718 gives an indication of the uncertainty of conventional bulk temperature measurements for
comparison with satellite-derived quantities, ignoring the surface skin effect. Those differentials
720 of more than 0.1°C were at on-station wind speeds of less than about 4 m/s (Figure 14 -- using
the hand-held anemometer 5 m above the sea surface).

722 Because bulk SSTs from merchant or research vessels will be drawn from deeper below
the water surface, the temperature differential between the near-surface (highest SDL

724 temperature) and the 3 m temperatures were also analysed (T0-T3; Figure 15). About 68% of the
temperature differences were less than 0.1°C and 83% were <0.3°C; the 8% of observations that
726 exceeded 0.5°C were all (with one exception) in November and December, before the strong
land- and sea-breezes of summer had set in.

728 Extending the analysis down to 18 m (the layer from which the depth-integrated
chlorophyll and nutrient samples were drawn), almost half the temperature differentials between
730 3 m and 18 m depth were <0.1°C and 75% were <0.3°C (Figure 15); 14% exceeded 0.5°C,
occurring mainly between December and January.

732 *4.6 Depth-integrated chlorophyll and nutrients*

The correlation between the spectrophotometric and fluorometric methods of measuring
734 the chlorophyll concentration was 0.92 (Figure 16), with higher values generally obtained from
the fluorometer. The fluorometric technique is 5 to 10 times more sensitive than the
736 spectrophotometric technique (Parsons et al., 1989), an important consideration given the
relatively low-chlorophyll waters off Western Australia (Pearce et al., 2000). The fluorometer
738 results will therefore be used in this paper.

By global standards, chlorophyll a levels were generally low (< 1 mg m⁻³; Figure 17) and
740 within the range of other chlorophyll data for Western Australian coastal waters (Department of
Environmental Protection, 1996; Pearce et al., 2000; Institute for Environmental Science, 2002).
742 The chlorophyll concentration was almost invariably higher within the coastal boundary layer
(stations H0 and H5) than further offshore; beyond station H10 the chlorophyll level rarely
744 exceeded 0.6 mg m⁻³ and indeed was often ≤ 0.3 mg m⁻³ (Figure 17). However, there was a high
degree of patchiness (Lord and Hillman, 1995), with little apparent seasonal pattern across the
746 two years; PLOOM sampling of chlorophyll a by Hale et al. (2001) has shown that chlorophyll
concentrations can vary an order of magnitude over a 24 hr period and by more than 0.1 ug/L
748 within 200 m distance. There were elevated chlorophyll levels right across the shelf in June
1998; the highest value measured during the entire project (2.3 mg m⁻³) was at H0. Yet in the

750 autumn/winter of the previous year (May and July 1997 -- there were no samples in June),
chlorophyll concentrations were uniformly low across the shelf, so any seasonality is perhaps
752 questionable from our results.

Chlorophyll measurements in the south-eastern Indian Ocean covering 5 degree
754 latitude/longitude squares (including adjacent to the Western Australian continental margin)
showed a clear winter peak (Humphrey, 1966), while Lourey et al. (2006) found summer
756 concentrations of about 0.25 mg m^{-3} rising to 1 mg m^{-3} in winter inshore of the Leeuwin Current,
attributing this seasonal increase either to terrestrial sources or through re-suspension of sandy
758 sediments in the shallow coastal waters during winter storms . A similar seasonal pattern was
evident in summer/winter sampling in Perth coastal waters in 1991/92 (Department of
760 Environmental Protection, 1996; Pearce et al., 2000). Satellite data from the Coastal Zone Color
Scanner (CZCS, which operated between 1979 and 1986 with some large data gaps off
762 southwestern Australia) also indicated that both the open-shelf and offshore chlorophyll
concentrations were higher between May and August than at other times of the year (Pearce et
764 al., 2000). However, there was a less distinct seasonal variation in a more recent study near the
Ocean Reef outlet (Figure 1; Thompson and Waite, 2003) where there were small chlorophyll
766 peaks in autumn and spring. We have re-examined the chlorophyll data from the 'control site'
south of the outlet and found that concentrations ranged from 0.01 to $2.68 \text{ mg chl a m}^{-3}$ but
768 without a clear seasonality.

The summer and winter SeaWiFS satellite chlorophyll images in Fearn et al. (submitted)
770 largely support the surface measurements, in particular the contrast between the low
concentrations in January 1998 and the elevated levels across the shelf in June 1998, as well as
772 the high level of fine-scale variability.

The nutrient dataset was limited to 16 months; all parameters (nitrate, phosphate and
774 silicate) showed considerable differences between the corresponding months for which data were
available. Nitrate and phosphate levels were usually highest within the coastal boundary layer

776 although there were a couple of pronounced mid-shelf peaks in nitrate in late 1997 (Figure
18a,b).

778 Because of the short time-series as well as the high level of variability, distinct seasonal
patterns were not evident. Both nitrate and phosphate were relatively high in late winter and
780 spring (September to December) of 1997; in mid-shelf and offshore regions, depth-integrated
nitrate ranged between 1.0 and 1.8 μM in a somewhat patchy distribution (Figure 18a).
782 Concurrently, phosphate reached a peak concentration of 0.29 μM in inshore waters, although
was elevated (0.20 – 0.25 μM) right across the shelf (Figure 18b). This contrasted with the same
784 period in 1998 when nitrate was almost uniformly < 0.2 μM (Figure 18a) and phosphate was
generally < 0.15 μM (Figure 18b), with the exception of the inshore waters. Overall, the 1998
786 nitrate results matched the seasonal pattern found earlier in the same coastal waters by Johannes
et al. (1994) who found monthly means of about 0.5 μM in summer rising to 1.5 μM in
788 June/July.

At the PLOOM site off Ocean Reef sampled between 1996 and 2001, nitrate sampling
790 (away from the immediate outlets) showed a broad winter peak concentration of about 2.5 μM
underlying a high degree of variability (Thompson and Waite, 2003), whereas longer-term
792 sampling further offshore (west of Rottnest Island, Figure 1) showed monthly mean nitrate
concentrations varying between 0.3 and 0.5 μM with no clear seasonal pattern (Pearce et al.,
794 1985). On the even broader scale of offshore waters, Lourey et al. (2006) found a small seasonal
signal with summer values of about 0.2 to 0.3 μM rising to 0.5 μM in winter but expressed
796 caution in interpreting seasonal patterns from parameters which fluctuate widely both spatially
and temporally.

798 Maximum silicate concentrations ($\geq 2.5 \mu\text{M}$) were primarily associated with offshore
waters and the autumn/winter period (Figure 18c). Mid-shelf and inshore waters showed
800 evidence of silicate depletion, especially during the summer of 1998 when there was a large mid-
shelf diatom bloom (Fearn et al., submitted) and silicate levels were drawn down below 1.5 μM

802 (Figure 18c). Diatom growth rates are thought to be limited at silicate concentrations below
approximately 2.0 μM (Dortch and Whitley, 1992), especially heavily silicified species such
804 as *Chaetoceros* (Trull et al., 2001). Silicate re-supply of shelf waters appears to come from
offshore, possibly via the Leeuwin Current which, based on recent analyses of nutrient
806 climatology for the region, may be a source of silicate (Lourey et al., 2006). High nitrate levels
in nearshore (2.1 μM) and mid-shelf (0.8 – 1.0 μM) waters during June 1998 coinciding with
808 replenished silicate concentrations from April and May 1998 may have been responsible for the
large cross-shelf diatom bloom evident both in cell counts (Fearn et al., submitted) and the
810 elevated cross-shelf chlorophyll mentioned above.

Local sewage outlets are known to contribute dissolved nutrients to the coastal waters,
812 increasing both water column productivity and chlorophyll concentrations (Thompson and
Waite, 2003). The nearest outlets to the Hillarys Transect are the Ocean Reef pipeline some 7 km
814 north of the Transect and Swanbourne 15 km to the south (Figure 1). During the PLOOM
monitoring program at the Ocean Reef outlet, nitrate levels were below 3 μM at the control site 4
816 km south of the outlet but peak individual values immediately above the outlet occasionally
exceeded 20 μM (Thompson and Waite, 2003). Those authors also found that there were slightly
818 elevated chlorophyll concentrations in spring and autumn. Since the highly elevated nutrient
concentrations were localised around the outlet site and did not extend more than about 4 km
820 from the outlets (Institute for Environmental Science, 2002), they would be unlikely to have
contributed to the nutrient spikes along the Hillarys Transect.

822 Although no regular measurements were made of chlorophyll and nutrient levels within
Hillarys Marina (Figure 1), occasional chlorophyll samples were taken for calibration purposes
824 within the Marina at the start of some Transects and tended to show elevated concentrations (see
for example the extreme point in Figure 16). An unpublished study of chlorophyll and nutrient
826 levels in the Marina between December 1999 and March 2000 showed highly variable
concentrations (Bowman Bishaw Gorham, 2001): chlorophyll a concentrations in the Marina

828 varied from 0.4 to 6.8 mg m⁻³ while at a station immediately outside the Marina entrance the
range was 0.5 to 2.5 mg m⁻³. Corresponding ranges of nitrate were 0.14 to 2.93 μM (in the
830 Marina) and 0.14 to 1.43 μM (entrance). Although this was only a brief summer study, it showed
that tidal outflow of high-chlorophyll Marina waters could contribute pulses of chlorophyll and
832 nutrients into the nearshore waters off Hillarys -- station H0 was only about 100 m outside the
Marina entrance.

834 Another source of nearshore nutrients is submarine groundwater discharge (SGD,
mentioned above) which is extremely high in nitrate levels (Johannes, 1980; Johannes and
836 Hearn, 1985) and may well be an important seasonal source of nutrients in Perth coastal waters,
although Lourey et al. (2006) suggest the effect may be rather localised in extent.

838 Although we sampled only the vertically-integrated water column (to a maximum of 18
m depth), vertical fluorescence profiles were measured by Fearn's et al. (submitted) on some
840 transects using a profiling fluorometer. In most cases, there was some "noise" in the upper 10 m
or so of the water column but typically thereafter the fluorescence was reasonably constant or
842 increased only slightly down to near the seabed. These profiles confirmed that the depth-
integrated sampling generally gave a good representation of the concentrations in the upper 18 m
844 layer. Historical data from a 3-year study of the water properties at stations in 10 and 22 m water
depth a few kilometres north of Hillarys (Pearce et al., 1985) showed that there was rarely any
846 consistent difference between surface and near-bottom nutrient samples. Similarly, Thompson
and Waite (2003) found no significant differences between surface and depth-integrated samples
848 at the PLOOM sites, and Hanson et al. (2005a) have shown that nitrate is often uniform down the
water column off the Capes (except when upwelling was occurring). Because of generally good
850 vertical mixing in this area and the relative shallowness of the water on the shelf, we believe that
the depth-integrated nutrients would be typical of the whole water column on most occasions,
852 especially at the shallower stations.

In summary, the high degree of nutrient and chlorophyll patchiness and the relatively
854 short time-series have tended to obscure any seasonal pattern in our results, but other studies
have (generally but not universally) indicated winter peaks in both nitrate & chlorophyll
856 concentrations.

4.7. *Horizontal small-scale surface variability*

858 Some of the uncertainties in validating satellite temperatures or chlorophyll
concentrations against surface in situ values are a result of the different kinds of measurement.
860 These include spot (i.e. single-point CTD sample) versus areal (satellite pixel) measurements
("within pixel" uncertainties), and navigation errors in the satellite or boat geolocation leading to
862 uncertainty in the pixel location ("between pixel" uncertainty). These can be examined using the
boat underway data at 1 km scales, the nominal pixel size for AVHRR and SeaWiFS products.
864 The underway measurements also revealed smaller-scale variability embedded within the larger-
scale cross-shelf temperature and chlorophyll structure discussed earlier.

866 The 1-km statistics (mean, standard deviation, maximum and minimum) were derived
from the underway SST and chlorophyll measurements (sampled at nominally 20 to 40 m
868 distance intervals) for both the outward and homeward runs in 1997 (SST only) and 1998.
Because there were sometimes "spikes" in SST or chlorophyll when the vessel stopped on station
870 and re-started, we have excluded the on-station positions from the analysis.

The highest variability was predictably within the coastal boundary layer inshore of
872 station H10 (Figure 19), encompassing the nearshore reef system where the water was shallowest
and the bathymetry most complex. However, weaker thermal and chlorophyll fronts were also
874 encountered further offshore with no clustering at any preferred sites.

Finer-scale frontal zones of order 0.5 to 1 °C were embedded within the gross cross-shelf
876 structure in both summer and autumn/winter (Figure 19). These fronts did not appear to group at
specific locations (except perhaps at the nearshore reef system), and so were presumably

878 associated more with the dynamics of the flow (such as the Leeuwin Current and the cross-shelf
tongues of water described earlier) than with any bathymetric features.

880 Chlorophyll patchiness was also evident. In December 1998 for example (Figure 19b),
there were two patches of relatively high chlorophyll water, one near the coast and the other mid-
882 shelf (this matched a small rise in the SST). Similar isolated patches of relatively high
chlorophyll water extending across 2 or 3 stations (5 to 15 km) were observed between April and
884 July 1998 at various positions on the shelf. Some (but certainly not all) of these were associated
with thermal fronts but their source is not immediately clear. Such surface chlorophyll peaks
886 may be associated with the filamentous cyanobacteria *Trichodesmium*, which is known to form
large surface slicks in Perth coastal waters (Institute for Environmental Science, 2002) and was
888 noted to be abundant at the Hillarys mid-shelf stations during December 1998 (Fearn et al.,
submitted).

890 The differences between the 1 km averages and the individual minima or maxima within
each 1 km segment enable an estimate to be made of the "within-pixel" variability when
892 comparing satellite SSTs and chlorophyll concentrations against spot in situ measurements.
From the 1997 and 1998 underway SST transects, 64% of the within-pixel differences were less
894 than 0.1°C and 93% less than 0.2°C (Figure 20a); very few differences exceeded 0.5°C. The
chlorophyll concentrations were more variable, but 85% of the differences were less than 0.05
896 mg m⁻³ (Figure 20b). Almost all the differences exceeding 0.1 mg m⁻³ were inshore of station H5
where the small-scale patchiness is greatest -- however, these shallow waters are unlikely to be
898 useful for satellite chlorophyll validation anyway because of bottom reflectance effects.

In a similar manner, uncertainties in SST or chlorophyll validation resulting from errors
900 in satellite geolocation can be assessed by examining the differences between adjacent 1-km
segments. For a positional error of 1 pixel, the SST differences between adjacent pixels were less
902 than 0.1°C for 68% of the observations and 87% were less than 0.2°C (Figure 21a); again, most
of the higher variability was close inshore. 57% of the chlorophyll differences were less than

904 0.02 mg m⁻³ and 86% within 0.05 mg m⁻³ (Figure 21b), but near the coast individual differences
sometimes exceeded 0.1 mg m⁻³.

906 These results provide an indication of the potential “error-bars” associated with natural
within-pixel variability when single point in situ validation measurements are compared with the
908 1 km pixel averages sensed by the satellite and with geolocation errors of one pixel; larger
geolocation uncertainties may have larger differences but are in fact unlikely for modern
910 remotely-sensed products. In summary, then, the uncertainties in validation of satellite SST due
to within-pixel and between-pixel variability combined is of order 0.4 °C while the uncertainties
912 for chlorophyll validation are of order 0.1 mg m⁻³.

4.8 Short-term temporal variability

914 There will be differences between the satellite and *in situ* temperatures associated with
the time interval between the surface measurements and the satellite overpass, as a result of both
916 air-sea heat flux (diurnal warming) and advection (see McAtee et al., this volume). The NOAA-
14 satellite was generally overhead in the early afternoon shortly after the Transect work had
918 been completed. Stratification in these shallow waters is very transient, breaking down over a
period of hours under sea-breeze conditions; Zaker et al. (2002) found that wind speeds of 6 m/s
920 were sufficient to vertically mix any diurnal stratification that develops. Nevertheless, the
shallow coastal waters would tend to warm more rapidly than the deeper water and so both
922 horizontal and vertical temperature differences can develop.

Some indication of typical warming trends during the day can be assessed using the
924 change in surface temperature at position H5 between the morning station (about 0930) and the
repeat station during the return leg some 4 hours later. The rise in bucket temperature was always
926 less than 1°C except for an isolated maximum of 1.3°C in March 1998, and a temperature
decrease of about 0.3°C in March and December 1997.

928 Because of the small number of station observations, a better estimate of the diurnal
heating may be obtained from the temperature sensor on the PCWS current meter 5 m below the

930 surface (discussed earlier). This showed that, on average, the daily lowest temperatures occurred
between 6 and 10 am, while the peak temperatures were from 3 to 8 pm; the mean diurnal
932 temperature range varied from 0.11°C in June to 0.39°C in February. Taking 10 am as the
approximate average time of the Transect stations and 2 pm as the time of the NOAA-14
934 overpasses, the differences between the bucket and satellite temperatures were less than 0.3°C on
89% of the days during the year, but about 1% of these differences were just over 0.5 °C.

936 4.9. *Interannual perspective*

There is a clear El Nino/Southern Oscillation (ENSO) signal along the Western
938 Australian coast (Pearce and Phillips, 1988, 1994), so a plot of the monthly Southern Oscillation
Index (SOI), the anomaly of Fremantle sea level and the Reynolds satellite-derived sea-surface
940 temperature (Reynolds and Smith, 1994) places the 27-month Hillarys Transect surveys in the
broader perspective.

942 The monthly or annual mean sea level at Fremantle has been used as a simple index of
the "strength" of the Leeuwin Current (originally proposed by Pearce and Phillips, 1988, and
944 subsequently confirmed and quantified by Feng et al., 2003): the higher the coastal sea level, the
greater is the cross-shelf slope and accordingly the stronger is the southward flow. The close link
946 between ENSO events and the Leeuwin Current is evident in Figure 22. During the prolonged
ENSO period in the early part of the decade, small negative values of the SOI were associated
948 with relatively low coastal sea levels and relatively low sea temperatures, implying a weak
Leeuwin Current between 1990 and 1995. The strong *La Nina* of 1996 (with higher sea levels, a
950 stronger Leeuwin Current and warmer water) was followed by the massive ENSO event of 1997,
succeeded in turn by the return to strong *La Nina* conditions towards the end of 1998.

952 Brief as the survey period was, the 1996-98 Hillarys Transects thus experienced a
complete cycle of a waning *La Nina*, a strong ENSO and a growing *La Nina*. While there were
954 some changes in the temperatures and salinities between the 2 years (Figure 9), these did not
affect the basic seasonality of the annual cycles. However, there were substantial differences in

956 the nutrient concentrations between the spring seasons of 1997 and 1998, and a much longer
monitoring programme will be required to establish any real interannual nutrient pattern that may
958 exist.

5. Summary of all results from the Hillarys Transect study

960 The field surveys off Hillarys between 1996 and 1998 have provided the first systematic,
multidisciplinary climatology of the physical, chemical and bio-optical properties across the
962 continental shelf in Southwestern Australia, as well as providing (near-) surface data for remote
sensing validation of sea-surface temperature and ocean colour. The study has also shown the
964 efficacy of using relatively simple methods to define the dominant oceanographic characteristics
of IMCRA coastal bioregions.

966 The major findings of the project, including the companion papers of McAtee et al. (this
volume), Fearn et al. (submitted) and Gaughan et al. (submitted) are:

968 5.1 Shelf water properties and cross-shelf exchange

* Seasonally-reversing temperature and salinity gradients across the continental shelf result from
970 both advective (Leeuwin Current, Capes Current) and air-sea flux processes. During the austral
spring and summer months of October to March, coastal heating and evaporation result in a band
972 of warmer and more saline water in a coastal boundary layer extending some 10 km offshore. In
winter by contrast, the warm, low salinity Leeuwin Current flows strongly southwards along the
974 shelfbreak, and the nearshore waters are much cooler (heat loss to the atmosphere) and less
saline (precipitation and freshwater input).

976 * The cross-shelf exchange (which has important implications for the exchange of plankton and
fish larvae between the Leeuwin Current and the coastal waters) is effected by 4 dominant
978 mechanisms: mesoscale meanders of the Leeuwin Current, smaller-scale tongues of Leeuwin
Current water penetrating across the continental shelf, high density nearshore waters episodically
980 cascading offshore down the seabed, and upwelling in the lee of Rottnest Island during the
summer months.

982 *5.2 Small-scale variability in relation to satellite measurements*

* Some of the uncertainties in comparing satellite and conventional surface temperatures in local
984 waters have been quantified using vertical temperature profiles and underway horizontal SST
sampling. The near-surface waters were usually well-mixed: for about 94% of the time there was
986 less than 0.2°C temperature difference in the uppermost metre of the water column (ignoring
surface "skin" effects).

* Differences between satellite-derived SSTs and in situ measurements can result from
horizontal small-scale ("within-pixel") patchiness. The underway measurements show that 93%
990 of the differences between individual samples and 1-km averages (representing an AVHRR
pixel) were less than 0.2°C -- this is effectively the potential "error" between the 1 km satellite
992 pixels and single-point in situ SST measurements.

* "Between-pixel" variability (such as from satellite geolocation errors) is shown by the
994 differences between adjacent 1-km block averages: SST differences between adjacent pixels
were less than 0.2°C for 87% of the observations offshore of the coastal boundary layer.

* Similarly, the underway fluorescence sampling (converted to chlorophyll by a regression
996 relationship) indicates that about 85% of within-pixel differences were less than 0.05 mg m⁻³
998 (again, outside the coastal boundary layer), and 86% of the "between-pixel" differences were less
than 0.05 mg m⁻³. The variability was much higher closer inshore.

* Comparisons between radiometer ("skin") temperatures and the satellite SSTs have shown
generally good agreement (especially at wind speeds exceeding 4 m/s), and match the cross-shelf
1002 and seasonal variability of the temperature field sampled by direct surface measurements
(McAtee et al., this volume). After correcting for time-of-day differences, the radiometer-
1004 satellite bias derived from individual monthly surveys varied between -1.5° and 0.2°C, with rms
differences between 0.4° and 1.7°C -- the higher values were all in late summer/early spring. The
1006 radiometer programme has emphasised the importance of careful instrument calibration and
accurate viewing angle for direct measurement of the skin SST.

1008 *5.3 Chlorophyll and nutrients*

* There was a high degree of both spatial and temporal “patchiness” in depth-integrated
1010 chlorophyll concentrations throughout the year, especially in the coastal boundary layer. Beyond
this nearshore band, the chlorophyll level rarely exceeded 0.6 mg m^{-3} and indeed was often < 0.3
1012 mg m^{-3} . Despite the patchiness and large interannual differences, there was a strong peak in
concentration right across the shelf in mid-winter 1998, but the seasonal cycle was less clearly
1014 defined close inshore than offshore.

* Chlorophyll concentrations derived from the SeaWiFS satellite (Fearn et al., submitted)
1016 largely supported the surface measurements along the Transect. The satellite estimates of surface
chlorophyll were generally within the 35% uncertainty specifications of the sensor in
1018 phytoplankton-dominated “Case 1” waters deeper than about 30 m, although the satellite values
may tend to under-estimate the true water column concentrations because of the deep chlorophyll
1020 maximum (DCM) at depths of 50 to 100 m (Hanson et al., 2005b).

* The SeaWiFS chlorophylls showed a winter peak matching that from the surface
1022 measurements. SeaWiFS estimates of the attenuation coefficient K_{490} were in good agreement
with KPAR values derived from the light profiles at mid-shelf and offshore stations, and peaked
1024 in the winter months (Fearn et al., submitted).

* Depth-integrated nitrate, phosphate and silicate concentrations showed considerable temporal
1026 and spatial variability, with the large differences between the corresponding months of the two
years sampled obscuring any clear seasonality. Nitrate and phosphate levels peaked between
1028 September and December 1997 in mid-shelf and offshore regions, but were almost uniformly
low in 1998 with the exception of inshore waters. Potential sources of nitrate include local
1030 submarine groundwater discharge (SGD), river effluent, local sewage outlets and the Marina
itself.

1032 * Maximum silicate concentrations were largely associated with offshore waters in
autumn/winter, while mid-shelf and inshore waters showed evidence of silicate depletion,
1034 especially during the summer months.

5.4 *Phyto- and zooplankton*

1036 * Although only limited phytoplankton sampling was undertaken and despite a high level of
temporal and spatial patchiness (Fearn et al., submitted), diatoms were found to be the most
1038 abundant group by far at all stations and throughout the year, followed by dinoflagellates and
cyanobacteria. Diatom density was highest in the mid-shelf region and tended to peak mid-year.
1040 The dinoflagellate and cyanobacteria distributions were less distinct, peaking in different seasons
and different positions along the mid-shelf region.

1042 * Macrozooplankton (Gaughan et al., submitted) were also patchy with a large variation between
the two years. The macrozooplankton community was characterised by a mixture of tropical and
1044 subtropical species (reflecting advection in the Leeuwin and Capes Current systems) but overall
densities were much lower than in the Benguela Current upwelling system.

1046 * Of the taxa processed, chaetognaths were dominant and were generally found inshore. The
numbers of chaetognath and siphonophore species and their abundances peaked in
1048 autumn/winter, while the distribution of pilchard eggs shows distinct spawning periods in both
summer and winter, concentrated in the mid-shelf region.

1050 * The source of an exceptionally high abundance of most taxa close inshore in May 1998 was
not evident, but the event clearly showed the high variability that can exist.

1052 5.5 *General comments*

Despite the simplicity of the methods used, this project has yielded some significant
1054 advances in our knowledge of the water properties and the plankton regime across the
continental shelf off Perth, and provides a good foundation for further work in this area.
1056 Inexpensive surveys of this type are adequate for defining the climatology of a coastal bioregion,
classifying its main characteristics and subsequently monitoring the water quality, but longer

1058 time-series (3 to 5 years -- see for example Pearce et al., 1985 and Thompson and Waite, 2003)
may be required to more adequately define the seasonal nutrient and chlorophyll cycles because
1060 of the high level of small-scale variability.

Because of the general sparsity of information along the Western Australian continental
1062 shelf, there is significant benefit in the utilisation of satellite-derived products for defining
baseline conditions, assessing natural variability and prescribing indicators of non-natural
1064 perturbations of the system due to such causes as climatic extremes or anthropogenic forcing.
This project has demonstrated that Chl-a concentration and diffuse attenuation coefficient,
1066 products often used as indicators of water quality and clarity, are able to be provided by remote
sensing methods, especially in open oceanic (case 1) waters where phytoplankton may be
1068 considered the dominant optically active constituent. Nearer the coast, when other constituents
are present in the water column, the assumptions on which the algorithms are based may be
1070 invalid so care must be taken in their utilisation.

For confidence in the remotely-sensed products right across the shelf into shallow coastal
1072 (Case 2) waters, robust measurements of water column properties are essential. These are
currently being undertaken through a new initiative (the Strategic Research Fund for the Marine
1074 Environment, or SRFME) which is investigating relationships between the oceanic environment,
primary productivity and zooplankton across the Western Australian continental shelf and out
1076 into deeper open-ocean water. While the dominant features of the seasonal and cross-shelf
distribution of the physical and optical water properties have been elucidated in the Hillarys
1078 Transects, more sophisticated sampling techniques and the greater geographic coverage in
SRFME will provide better in situ validation data especially in the nearshore (Case 2) waters.

Acknowledgements

- * Fisheries Research and Development Corporation (FRDC) for funding support.
- * Perth Diving Academy (PDA) for leasing the *Lionfish 2* at very reasonable rates and for much-appreciated assistance from the crew during the surveys.
- * Glenn Cooke and John Cramb (Bureau of Meteorology) for wind data from the Rottneest AWS and for seasonal wind roses.
- * DA Lord and Associates (now Oceanica Consulting), the Centre for Water Research (University of Western Australia) and Steedman Science and Engineering (now Metocean Engineers) for PCWS current meter data.
- * The Western Australian Satellite Technology and Applications Consortium (WASTAC) for NOAA and SeaWiFS satellite imagery.
- * Salinity data from the Swanbourne PLOOM sampling sites were kindly provided by Mark Nener (Water Corporation). The data were collected by Murdoch University Marine and Freshwater Research Laboratory (MAFRL) and Oceanica Consulting.
- * Rose Lerch (Department of Water, Perth) for Swan River streamflow data.
- * Ben Hollyock (RPS Bowman Bishaw Gorham) for water quality data from Hillarys Marina.
- * Simon Braine (CSIRO Marine Research) and Luke Twomey (Curtin University) for the chlorophyll sampling and laboratory analyses.
- * Bob Griffiths, Neale Johnston and Val Latham (CSIRO Marine Research) for salinity and nutrient analyses.
- * Students from the Remote Sensing and Satellite Research Group at Curtin University who very ably assisted during the field surveys and data processing/analysis.

This paper is dedicated to the memory of Wilma Vincent.

References

- Alaee, M.J., 1998. Dynamics of island wakes on continental shelves. Unpublished Ph.D thesis, University of Western Australia, 149pp.
- Alaee, M.J., Pattiaratchi, C.B., Ivey, G., 1998. A field study of the three-dimensional structure of the Rottnest Island wake. *In: Physics of Estuaries and Coastal Seas*, ed. Dronkers and Scheffers, Balkema, Rotterdam, 239-245.
- Bowman Bishaw Gorham (2001). Port Catherine Environmental Review Volume 2 – Appendix IV: Marine water quality assessment. Unpublished report prepared for Western Australian Planning Commission, Perth.
- Breckling, J., 1989. The analysis of directional time series: applications to wind speed and direction. *Lecture Notes in Statistics 61*, Springer-Verlag, Berlin, 238pp.
- Bureau of Meteorology, 1966. Climatic survey region 15 – metropolitan Western Australia. Bureau of Meteorology (Australia), Melbourne, 164pp.
- CALM, 1992. Marmion Marine Park Management Plan 1992-2002. Management Plan No 23. Department of Conservation and Land Management for the National Parks and Nature Conservation Authority. Perth, Western Australia, Australia.
- Caputi, N., Fletcher, W.J., Pearce, A.F, Chubb, C.F., 1996. Effect of the Leeuwin Current on the recruitment of fish and invertebrates along the West Australian coast. *Proceedings of the International Larval Fish Conference*, June 1995; *Marine and Freshwater Research* 47, 147-155.
- Colborn, J.G., 1975. The thermal structure of the Indian Ocean. University Press of Hawaii, Honolulu, 173pp.

- Cowley, R., Critchley, G., Eriksen, R., Latham, V., Plaschke, R., Rayner, M., Terhell, D., 1999. Hydrochemistry Operations Manual. CSIRO Marine Research Report 236, 106pp.
- Cresswell, G.R., 1980. Satellite-tracked buoys in the the eastern Indian Ocean. Proceedings of the 14th International Symposium on Remote Sensing of the Environment Costa Rica April 1980, 531-541.
- Cresswell, G.R., 1991. The Leeuwin Current -- observations and recent models. Proceedings of the Leeuwin Current Symposium. Journal of the Royal Society of Western Australia 74, 1-14.
- Cresswell, G., 1996. The Leeuwin Current near Rottnest Island, Western Australia. Marine and Freshwater Research 47, 483-487.
- Cresswell, G.R., Boland, F.M., Peterson, J.L., Wells, G.S., 1989. Continental shelf currents near the Abrolhos Islands, Western Australia. Australian Journal of Marine and Freshwater Research 40, 113-128.
- Cresswell, G.R., Griffin, D.A., 2004. The Leeuwin Current, eddies and sub-Antarctic waters off south-western Australia. Marine and Freshwater Research 55, 267-276.
- Cresswell, G.R., Peterson, J.L., 1993. The Leeuwin Current south of Western Australia. Australian Journal of Marine and Freshwater Research 44, 285-303.
- Department of Environmental Protection, 1996. Southern Metropolitan Coastal Waters Study (1991-1994) Final Report. Western Australian Department of Environmental Protection Report 17, 288pp.

- Dortch, Q. and Whittedge, T. E., 1992. Does nitrogen or silicon limit phytoplankton production in the Mississippi River plume and nearby regions? *Continental Shelf Research* 12, 1293-1309.
- Dunlop, J.N., Wooller, R.D., 1990. The breeding seabirds of Southwestern Australia: trends in species, populations and colonies. *Corella* 14, 107-112.
- Environment Australia, 1998. Australia's oceans policy: caring, understanding, using wisely, Australia's oceans. Commonwealth of Australia, Oceans Policy Marine Group, 52pp.
- Fearn, P.R., Twomey, L., Zakiyah, U., Hellen, S., Vincent, W., Lynch, M.J., submitted. The Hillarys transect (3): Optical and chlorophyll relationships across the continental shelf off Perth. Submitted to *Continental Shelf Research*.
- Feng, M., Meyers, G., Pearce, A., Wijffels, S., 2003. Annual and interannual variations of the Leeuwin Current at 32°S. *Journal of Geophysical Research* 108(C11), 3355, doi:10.1029/2002JC001763, 2003.
- Gaughan, G.J., Pearce, A.F., Lewis, P., submitted. Influences on the seasonal variability of chaetognaths and siphonophores on the continental shelf off Perth, Western Australia. Submitted to *Estuarine, Coastal and Shelf Science*.
- Gaughan, D.J., Potter, I.C., 1994. Relative abundance and seasonal changes in the macrozooplankton of the lower Swan Estuary in South-western Australia. *Records of the West Australian Museum* 16, 461-474.
- Gentili, J., 1971. *Climates of Australia and New Zealand*. World Survey of Climatology, Elsevier Publishing Company, Amsterdam, 405pp.

- Gersbach, G.H., Pattiaratchi, C.B., Ivey, G.N., Cresswell, G.R., 1999. Upwelling on the south-west coast of Australia -- source of the Capes Current? *Continental Shelf Research* 19, 363-400.
- Godfrey, J.S., Ridgway, K.R., 1985. The large-scale environment of the poleward-flowing Leeuwin Current, Western Australia: longshore steric height gradients, wind stresses and geostrophic flow. *Journal of Physical Oceanography* 15, 481-495.
- Gray, C.A., Kingsford, M.J., 2003. Variability in thermocline depth and strength, and relationships with vertical distributions of fish larvae and mesozooplankton in dynamic coastal waters. *Marine Ecology Progress Series* 247, 211-224.
- Greig, M.A., 1986. The 'Warreen' sections: temperatures, salinities, densities and steric heights in the Leeuwin Current, Western Australia, 1947-1950. *CSIRO Marine Laboratories Report* 175, 22pp.
- Griffin, D.A., Wilkin, L.J., Chubb, C.F., Pearce, A.F., Caputi, N., 2001. Mesoscale oceanographic data analysis and data assimilative modelling with application to Western Australian fisheries. Final report on Project 97/139 to the Fisheries Research and Development Corporation (FRDC), 52pp.
- Hale, J., Hellen, S., Paling, E.I., 2001. Perth long-term ocean outlet monitoring. Project E2: phytoplankton (1996 to 2001). Unpublished report MAFRA 01/6, Institute for Environmental Science, Murdoch University, 92pp.
- Hamilton, L.J., 1986. Statistical features of the oceanographic area off south-western Australia obtained from bathythermograph data. *Australian Journal of Marine and Freshwater Research* 37, 421-436.

- Hanson, C.E., Pattiaratchi, C.B., Waite, A.M., 2005a. Seasonal production regimes off south-western Australia: influence of the Capes and Leeuwin Currents on phytoplankton dynamics. *Australian Journal of Marine and Freshwater Research* 56, 1011-1026.
- Hanson, C.E., Pattiaratchi, C.B., Waite, A.M., 2005b. Sporadic upwelling on a downwelling coast: phytoplankton responses to spatially variable nutrient dynamics off the Gascoyne region of Western Australia. *Continental Shelf Research* 25, 1561-1582.
- Hatcher, B.G., 1991. Coral reefs in the Leeuwin Current -- an ecological perspective. *Proceedings of the Leeuwin Current Symposium. Journal of the Royal Society of Western Australia* 74, 115-127.
- Humphrey, G.F., 1966. The concentration of chlorophylls a and c in the south-east Indian Ocean. *Australian Journal of Marine and Freshwater Research* 17, 135-145.
- Hutchins, J.B., 1991. Dispersal of tropical fishes to temperate seas in the southern hemisphere. *Journal of the Royal Society of Western Australia* 74, 79-84.
- Hutchins, J.B., 1999. Mortality of *Pocillopora* coral at Rottnest Island, Western Australia. In: Walker, D.I., Wells, F.E. (Eds.), *The seagrass flora and fauna of Rottnest Island, Western Australia*. Western Australian Museum, Perth, pp. 281-293.
- Hutchins, J.B., Pearce, A.F., 1994. Influence of the Leeuwin Current on recruitment of tropical reef fishes at Rottnest Island, Western Australia. *Bulletin of Marine Science* 54, 245-255.

- IMCRA, 1998. Interim Marine and Coastal Regionalisation for Australia: An ecosystem-based classification for marine and coastal environments. IMCRA Technical Group, Commonwealth Department of the Environment, Canberra, Australia.
- Institute for Environmental Science, 2002. Perth long term ocean outlet monitoring: phytoplankton monitoring programme (1996 to 2002). Murdoch University Institute for Environmental Science Report MAFRA 02/5 to DAL Science and Engineering, 87pp.
- Johannes, R.E., 1980. The ecological significance of the submarine discharge of groundwater. *Marine Ecology - Progress Series* 3, 365-373.
- Johannes, R.E., Hearn, C.J., 1985. The effect of submarine groundwater discharge on nutrient and salinity regimes in a coastal lagoon off Perth, Western Australia. *Estuarine, Coastal and Shelf Science* 21, 789-800.
- Johannes, R.E., Pearce, A.F., Wiebe, W.J., Crossland, C.J., Rimmer, D.W., Smith, D.F., Manning, C.R., 1994. Nutrient characteristics of well-mixed coastal waters off Perth, Western Australia. *Estuarine Coastal and Shelf Science* 39, 273-285.
- Legeckis, R., Cresswell, G., 1981. Satellite observations of sea-surface temperature fronts off the coast of western and southern Australia. *Deep-Sea Research* 28A, 297-306.
- Lenanton, R.C., Joll, L., Penn, J., Jones, K., 1991. The influence of the Leeuwin Current on coastal fisheries of Western Australia. *Journal of the Royal Society of Western Australia* 74, 101-114.
- Longhurst, A., 1995. Seasonal cycles of pelagic production and consumption. *Progress in Oceanography* 36, 77-167.

- Lord, D.A., Hillman, K., 1995. Perth Coastal Waters Study: Summary Report. Report to the Water Authority of Western Australia, 134pp.
- Lourey, M.J., Dunn, J.R., Waring, J., 2006. A mixed-layer nutrient climatology of Leeuwin Current and Western Australian shelf waters: seasonal nutrient dynamics and biomass. *Journal of Marine Systems* 59, 25-51.
- Masselink, G., Pattiaratchi, C.B., 2001. Characteristics of the sea breeze system in Perth, Western Australia, and its effect on the nearshore wave climate. *Journal of Coastal Research* 17, 173-187.
- Maxwell, J.G.H., Cresswell, G.R., 1981. Dispersal of tropical marine fauna to the Great Australian Bight by the Leeuwin Current. *Australian Journal of Marine and Freshwater Research* 32, 493-500.
- McAtee, B.K., Pearce, A.F., Lynch, M.J., Davies, J., Boterhoven, M., Osborne, B.J. (this volume). The Hillarys transect (2): Validation of satellite-derived sea-surface temperature in the Indian Ocean off Perth, Western Australia. Submitted to *Continental Shelf Research*.
- McMillin, L.M., Crosby, D.S., 1984. Theory and validation of the multiple window sea surface temperature technique. *Journal of Geophysical research* 89, 3655-3661.
- Mills, D.A., D'Adamo, N., Wyllie, A., Pearce, A.F., 1996. The response of stratified shelf waters to the Leeuwin Current and wind forcing: winter observations off Perth, Western Australia. *In: Mixing in Estuaries and Coastal Seas, Coastal and Estuarine Studies Volume 50* (ed. C.Pattiaratchi), American Geophysical Union, 5-28.
- Neumann, G., 1968. *Ocean Currents*. Elsevier Scientific Publishing Company, Amsterdam, 352pp.

- Parsons, T. R., Maita, Y., Lalli, C. M., 1989. A manual of chemical and biological methods for seawater analysis, pp. 173. Toronto: Pergamon Press.
- Pattiaratchi, C.B., Imberger, J., Zaker, N., Svenson, T., 1995. Perth Coastal Waters Study: physical measurements. University of Western Australia, Centre for Water Research Report WP947CP to the Water Authority of Western Australia, 57pp + Figures and Appendices.
- Pearce, A.F., Phillips, B.F., Crossland, C.J., 1992. Larval distributions across the Leeuwin Current: report on RV *Franklin* cruise Fr8/87 in August/September 1987. CSIRO Marine Laboratories Report 217, 13pp.
- Pearce, A.F., 1997. The Leeuwin Current and the Houtman Abrolhos Islands. *In*: Wells F. E. (editor), The marine flora and fauna of the Houtman Abrolhos Islands, Western Australia. Proceedings of the 7th International Marine Biology Workshop, Western Australian Museum, Volume 1, 11-46.
- Pearce, A.F., Griffiths, R.W., 1991. The mesoscale structure of the Leeuwin Current: a comparison of laboratory models and satellite imagery. *Journal of Geophysical Research* 96, 16739-16757.
- Pearce, A.F., Hellen, S.K.R., Marinelli, M., 2000. Review of productivity levels of Western Australian coastal and estuarine waters for mariculture planning purposes. Fisheries WA Research Report No.123, 67pp.
- Pearce, A.F., R.E.Johannes, C.R.Manning, D.W.Rimmer, and D.F.Smith 1985. Hydrology and nutrient data off Marmion, Perth: 1979-1982. CSIRO Marine Laboratories Report 167, 46p.

- Pearce, A.F., Pattiaratchi, C.B., 1999. The Capes Current: a summer countercurrent flowing past Cape Leeuwin and Cape Naturaliste, Western Australia. *Continental Shelf Research* 19, 401-420.
- Pearce, A.F., Phillips, B.F., 1988. ENSO events, the Leeuwin Current and larval recruitment of the Western Rock Lobster. *Journal du Conseil* 45, 13-21.
- Pearce, A.F., Phillips, B.F., 1994. Oceanic processes, puerulus settlement and recruitment of the western rock lobster *Panulirus cygnus*. In Sammarco, P.W. and M.L.Heron (editors): *The bio-physics of marine larval dispersal*. American Geophysical Union, Coastal and Estuarine Studies 45, Washington DC., 279-303.
- Qu, T., 2001. Role of ocean dynamics in determining the mean seasonal cycle of the South China Sea surface temperature. *Journal of Geophysical Research* 106, 6943-6955.
- Reynolds, R.W., Smith, T.M., 1994. Improved global sea surface temperature analyses using optimal interpolation. *Journal of Climate* 7, 929-948.
- Robinson, I.S., Wells, N.C., Charnock, H., 1984, The sea surface thermal boundary layer and its relevance to the measurement of sea surface temperature by airborne and spaceborne radiometers. *International Journal of Remote Sensing*, 5, 19-45.
- Rochford, D.J., 1969. Seasonal variations in the Indian Ocean along 110°E. 1. Hydrological structure of the upper 500 m. *Australian Journal of Marine and Freshwater Research* 20, 1-50.
- Rochford, D.J., 1980. Nutrient status of the oceans around Australia. CSIRO Division of Fisheries and Oceanography Report 1977-79, 9-20.

- Rochford, P.A., Kindle J.C., Gallacher, P.C., Weller, R.A., 2000. Sensitivity of the Arabian Sea mixed layer to 1994-1995 operational wind products. *Journal of Geophysical Research* 105, 14141-14162.
- Shapiro, G. I., Huthnance, J. M., Ivanov, V. V., 2003. Dense water cascading off the continental shelf. *Journal of Geophysical Research* 108(C12), 3390, doi:10.1029/2002JC001610.
- Smith, R.L., Huyer, A., Godfrey, J.S., Church, J.A., 1991. The Leeuwin Current off Western Australia, 1986-1987. *Journal of Physical Oceanography* 21, 323-345.
- Steedman, R.K. and Associates, 1981. Cape Peron waste water ocean outlet effluent dispersion studies. Unpublished Steedman and Associates Report R124 to Binnie and Partners Pty, Ltd.
- Steedman, R.K., Craig, P.D., 1983. Wind-driven circulation of Cockburn Sound. *Australian Journal of Marine and Freshwater Research* 34, 187-212.
- Symonds, G., Gardiner-Garden, R., 1994. Coastal density currents forced by cooling events. *Continental Shelf Research* 14, 143-157.
- Thompson, P., Waite, A., 2003. Phytoplankton responses to wastewater discharges at two sites in Western Australia. *Marine and Freshwater Research* 54, 721-735.
- Trull, T., Rintoul, S. R., Hadfield, M. Abraham, E. R., 2001. Circulation and seasonal evolution of polar waters south of Australia: implications for iron fertilization of the Southern Ocean. *Deep-Sea Research II* 48, 2439-2466.
- Watts, L.J., Owens, N.J.P., 1999. Nitrogen assimilation and the f-ratio in the northwestern Indian Ocean during an intermonsoon period. *Deep-Sea Research II* 46, 725-743.

- Wells, M. G., Sherman, B., 2001). Stratification produced by surface cooling in lakes with significant shallow regions. *Limnology and Oceanography* 46, 1747-1759.
- Woo, M., Pattiaratchi, C., Schroeder, W., 2006. Summer surface circulation along the Gascoyne continental shelf, Western Australia. *Continental Shelf Research* 26, 132-152.
- Wyllie, A., Buchanan, A., D'Adamo, N., Mills, D., Pearce, A., 1992. The use of Landsat Thematic Mapper and NOAA AVHRR for environmental investigations of the Perth metropolitan coastal waters. *Proceedings of the 6th Australasian Remote Sensing Conference*. Wellington, New Zealand, pp. 203-208.
- Zaker, N.H., Imberger, J., Pattiaratchi, C.B., 2002. Numerical simulation of the coastal boundary layer off Perth, Western Australia. *Journal of Coastal Research* 18, 470-485.
- Zaker, N.H., Imberger, J., Pattiaratchi, C.B., submitted. Dynamics of the coastal boundary layer off Perth, Western Australia. Submitted to *Continental Shelf Research*.

Figure Captions

Figure 1: The continental shelf region of southwestern Australia, showing the location of the Hillarys Transect (filled circles, stations H0 to H40), Hillarys Marina with a weather station (HM) and the mouth of the Swan River (SR). The Swanbourne and Ocean Reef waste outlets are SW and OC respectively, and the CSIRO "Rottnest station" is ROT. The alongshore transect stations A to S (filled squares) are described in the text. The arrows depict a representation of the Leeuwin (warm water, solid arrows) and Capes (cooler water, dashed arrows) Currents. The bathymetry has been simplified from the National Bathymetric Survey 1:250,000 Series chart "Yanchep".

Figure 2: Seasonal wind roses for the Rottnest Island AWS, covering the period late 1987 to early 2006, courtesy of John Cramb, Bureau of Meteorology, Perth. The seasons are defined as December-January-February (southern hemisphere summer) etc, and the 9 am and 3 pm roses are presented separately because of the dominant sea-breeze pattern in the summer months. Directions are in the traditional meteorological sense, i.e. direction from which the wind is blowing. The wind speed and frequency scales are indicated in the attached box.

Figure 3: Monthly mean alongshore current components at mid-depth at (a) the PCWS joined deep water mooring sites DW1 + DW2 (in 220 m and 110 m water depths respectively; the change occurred in March 1993) and (c) the shallow water mooring SW2 (in 27 m water); northward flow is positive. Figures (b) and (d) show the relative frequencies of northwards (solid bars) and southwards (pale bars) currents, defined by the sectors NW to NE and SW to SE respectively, at the deep and shallow water sites. Data courtesy of DA Lord and Associates (now Oceanica Consulting), the Centre for

Water Research (University of Western Australia) and Steedman Science and Engineering (now Metocean Engineers).

Figure 4: Bathymetric profile along the Hillarys Transect derived from an echosounding run (out to H40) and thereafter from the National Bathymetric Survey 1:250,000 Series chart "Yanchep". The dropped lines show the station positions H0 to H40.

Figure 5: Monthly mean wind vectors and wind components over the 3-year period 1996 to 1998 from the Rottneest Island weather station operated by the Australian Bureau of Meteorology. Both the wind vectors and the components are in the direction towards which the wind is blowing. The stability is defined in the text.

Figure 6: NOAA-AVHRR satellite images of sea-surface temperature off Perth in January 1997 (upper panel, representing summer conditions) and July 1997 (lower panel, winter). The warmest water is depicted as red, cooling through yellow and green to the coolest water in blue; the images have been individually colour-enhanced to show greatest detail of the thermal structure so the colours do not match between the two images. The temperatures are the brightness temperatures in AVHRR band 4, and have not been corrected for atmospheric effects. The black contour marks the position of the 200 m isobath, approximately delineating the edge of the continental shelf, and the Hillarys Transect is the solid line partly crossing the shelf.

Figure 7: Digital AVHRR SST transects from 113°E to the coast in January 1997 (upper curve -- summer) and July 1997 (lower curve -- winter), matching the images in Figure 6. The Hillarys Transect is shown by the H40-H0 bar at the top of the Figure, and the squares and triangles represent the SDL temperatures at the Transect stations. The vertical line marks the approximate position of the 200 m isobath ("shelf-break").

The southward-flowing Leeuwin Current is visible in each season (circles with dots) while the cool Capes Current and the warm eddy (derived from the Leeuwin Current) are northward currents (circles with crosses).

Figure 8: NOAA-AVHRR satellite images of sea-surface temperature off Perth in January 1998 (upper panel) and October 1998 (lower panel). Details as in Figure 6.

Figure 9: Time-distance contour diagrams of (a) surface temperature and (b) surface salinity along the Hillarys Transect between October 1996 and December 1998. The dots show the station positions.

Figure 10: Monthly mean (a) surface temperature and (b) salinity near the coast (stations H0 and H5 -- filled circles) and offshore (stations H35 and H40 -- open circles) derived from the 27 monthly transects. The minima and maxima measured in each calendar month are also indicated.

Figure 11: Temperature/salinity (T/S) diagram for surface temperatures and salinities at all stations between 1996 and 1998. The blocked areas depict the approximate characteristics of the seasonal water properties defined in the text.

Figure 12: Surface salinities sampled at stations A to S (Figure 1) between 1985 and 1989 (CSIRO unpublished data), collapsed into a single year. Salinities below 32 psu have been omitted to show more detail of the finer-scale differences above 35 psu.

Figure 13: (a) to (d) Examples of the vertical temperature structure across the continental shelf derived from the SDL profiles. See text for explanation.

Figure 14: Relationship between the near-surface temperature differential (between the highest SDL temperature SDL_{max} and the average temperature T_1 in the top 1 m of the water column) and the on-station wind speed measured with the hand-held anemometer.

Figure 15: Histogram of SDL profile temperature differences between the surface and 3 m depth (solid bars) and 3 m to 18 m depth layer (clear bars), derived from the SDL 1-m depth-interval temperature profiles.

Figure 16: Scatterplot of the chlorophyll-a concentration derived using the spectrophotometric method (horizontal axis) and the fluorometric technique (vertical axis).

Figure 17: Time-distance contour diagrams of depth-integrated chlorophyll-a concentrations along the transect between October 1996 and December 1998, measured by the fluorometer. The dots show the station positions; there were no samples in June 1997, and the August 1998 transect was truncated due to poor weather.

Figure 18: Time-distance contour diagrams of depth-integrated concentrations of (a) nitrate, (b) silicate and (c) phosphate across the transect between September 1997 and December 1998. The dots show the station positions; the August 1998 transect was truncated due to poor weather. Some of the nitrate concentrations were below the 0.03 μM analytical threshold and so are classified as zeros.

Figure 19: Along-transect 1-km averaged surface temperature (filled circles) and fluorescence/chlorophyll (open circles) in (a) May and (b) December 1998 from the underway measurements. The envelopes mark the \pm standard deviation limits in each case.

Figure 20: Histograms of the along-transect 1-km (within-pixel) variability showing the mean - minimum/maximum differences for (a) SST and (b) chlorophyll derived from the underway measurements. The SSTs are for the full period 1996 to 1998, while the chlorophylls are for 1998 only.

Figure 21: Histograms of the along-transect between-pixel variability showing the differences between adjacent 1 km segments for (a) SST and (b) chlorophyll derived from the underway measurements. The SSTs are for the full period 1996 to 1998, while the chlorophylls are for 1998 only.

Figure 22: Monthly values of the Southern Oscillation Index (SOI -- small dots), Fremantle sea level anomaly (FMSL -- filled circles) and the Reynolds SST anomaly for the 1-degree square 31°-32°S and 115°E to the coast (SST -- open circles) between 1990 and 1998. The anomalies have been derived by subtracting each individual monthly value from the long-term mean for that month, and smoothed by a simple 5-month moving average to reduce smaller-scale variability. The Hillarys Transects covered the last 27 months.